Stony Brook University

Regenerative Shock Absorbers for Energy Harvesting from Vehicle Suspensions

A Thesis Presented

by

Zhongjie Li

to

The Graduate School

in Partial Fulfillment of the

Requirements

for the Degree of

Master of Science

in

Mechanical Engineering

Stony Brook University

August 2012

Stony Brook University

The Graduate School

Zhongjie Li

We, the thesis committee for the above candidate for the

Master of Science degree, hereby recommend

acceptance of this thesis.

Zuo, Lei – Thesis Advisor
Assistant Professor in Mechanical Engineering

Kao, Imin – Chairperson of Defense
Associate Dean in College of Engineering and Applied Sciences

Longtin, Jon – Committee Member
Associate Professor in Mechanical Engineering

Babajimopoulos, Aristotelis – Committee Member
Assistant Professor in Mechanical Engineering

This thesis is accepted by the Graduate School

Charles Taber
Interim Dean of the Graduate School

Abstract of the Thesis

Regenerative Shock Absorbers for Energy Harvesting from Vehicle Suspensions

by

Zhongjie Li

Master of Science

in

Mechanical Engineering

Stony Brook University

2012

While the energy consumption around the world is keeping increasing, energy harvesting is more and more popular, especially in vehicle suspensions. The objective of this research is to design an electricity-harvesting shock absorber with high-power density and retrofittability to recover large amount of vibration energy traditionally dissipated in vehicle suspensions and to enhance vehicle dynamics for ride comfort and road safety at the same time.

An introduction and overview of vehicle suspensions as well as regenerative shock absorbers is presented to help understand the motivation for the research. 100 to 400 Watts' energy is accessible in vehicle suspensions, which corresponds to 1-6% increase in fuel efficiency. However, current regenerative shock absorbers' energy density is low and they cannot fit in vehicles. As a result, this research is focused on increasing energy density and decreasing dimensions.

In order to understand the relationship between the design parameters and dynamic performances of regenerative shock absorbers, a dynamic model for a rack-pinion type regenerative shock absorber has been derived and analyzed based on differential equations. To understand the influence of the friction and backlash on the system, nonlinear models have been created. Simulations are carried out to study the features of the design. The validation of the models is demonstrated by comparing the simulation

results with experimental measurements. Guidelines are given for the design of this type of regenerative shock absorbers.

Based on the guidelines, an improved design of a retrofit regenerative shock absorber is prototyped and tested. Results show that variable damping coefficients and asymmetric feature in jounce and rebound motions are achieved by controlling the electrical load of the shock absorber. Improved efficiency and reliability are achieved by utilizing a roller to guide the rack and preload on the gear transmission to reduce the backlash and friction. A peak power of 68 Watts is attained from one prototype shock absorber when the vehicle is driven at 30 mph on a fairly smooth campus road.

To keep improving the regenerative shock absorbers' reliability and efficiency, an innovative design of regenerative shock absorbers is proposed, with the advantage of significantly improving energy harvesting efficiency and reducing the impact forces caused by oscillation. The key component is a unique motion mechanism, which is called "mechanical motion rectifier", to convert the suspension's oscillatory vibration into unidirectional rotation of the generator. An implementation of motion rectifier based harvester with high compactness is introduced and prototyped. A dynamic model is created to analyze the general properties of the motion rectifier by making analogy between mechanical systems and electrical circuits. The model is capable of analyzing electrical and mechanical components at the same time. Both simulation and experiments are carried out to verify the modeling and the advantages. The prototype achieved over 60% efficiency at high frequency, much better than the conventional regenerative shock absorbers in oscillatory motion. The motion rectifier based design can also be used for other applications of electromagnetic vibration energy harvesting.

A ball screw based "Mechanical Motion Rectifier" is also presented with design calculation and models because the ball screw is more reliable than rack pinion mechanism. However, there are possibly some dead zones with wrong design parameters. So, the dead zones are modeled and analyzed, and design guidelines are provided for avoiding dead zones in the future designs.

The regenerative shock absorbers can not only harvest energy from vehicle vibrations, but also provide better performances with controllers. The combination of "mechanical

motion rectifier” and regenerative shock absorbers improves the reliability and efficiency at the same time, which makes regenerative shock absorbers more practical and functional.

Key Words: *energy harvesting, regenerative shock absorber, vehicle suspension, mechanical motion rectifier*

Table of Contents

List of figures

List of tables

Acknowledgements

I would like to thank my supervisor, Prof. Lei Zuo, for his help and support, and for teaching how to do good research. This project would not have been possible without his dedication.

In addition, I would like to thank Prof. Imin Kao, Prof. Jon Longtin and Prof. Aristotelis Babajimopoulos, for being a part of my thesis committee.

I would also like to thank the people who provided great help in this project, including Mr. David McAvoy and James T. O'Connor of SBU Dransportation Department, Prof. Yixian Qin and Liangjun Lin of SBU BME department for providing the testing facilities, Zachary Brindak, Xiudong Tang, Peng Li, Teng Lin, Wanlu Zhou, John Wang, Yilun Liu, and Yusong Di for assistance I received in my research.

Last, but not least, I would thank my family for their consistant support and encouragement.

Sincerely

Chapter 1 introduction

1.1 Motivation

Automobiles are utilized all around the world and provide their users with a highly convenient means of transportation. Despite their benefits, automobiles, in general, are a significant contributor to the energy and environment issues that we are facing today. In the United States, automobiles are responsible for 40% of all oil consumption[1]; yet only 10-16% of that fuel energy is used to actually drive the vehicle (to overcome the resistance from road friction and air drag) [2]. Vehicles dissipate (waste) a large portion of their energy in the form of kinetic energy through their braking and suspension systems.

As the consistently increasing oil price, energy harvesting from wasted energy in vehicles is more and more important. Figure 1.1 shows around 10% percent fuel efficiency can potentially be improved with regenerative shock absorbers. Considering there are 255.9 million registered vehicles in the United States, including passenger cars and light trucks according to the statistics of US DOT in 2008. Suppose vehicles are driven around one hour per day and we harvest the vehicle vibration energy at 400 Watts, we can continuously save the energy at rate of

255,900,000 X 1 hour X 400 Watts/24 hours = 4.26 Giga Watts

This doesn't include the 0.56 million railcars and the military vehicles. It is still larger than the capacity of the Niagara Power Plant (1.47GW), one of the largest hydroelectric power stations in the US.

The total electricity in one year will be

255,900,000 X 1 hour/day X 400 Watts X 365 days= 37.4 billion kW-H.

Using the electricity price 10.8 cents per kW-H of transportation sector (US DOE data) and average electricity source emission 1.37 lbs CO_2 per kW-H (US DOE data), the economic benefit will be 4.1 billion US dollars, and the annual green gas reduction is 25.6 million tons.

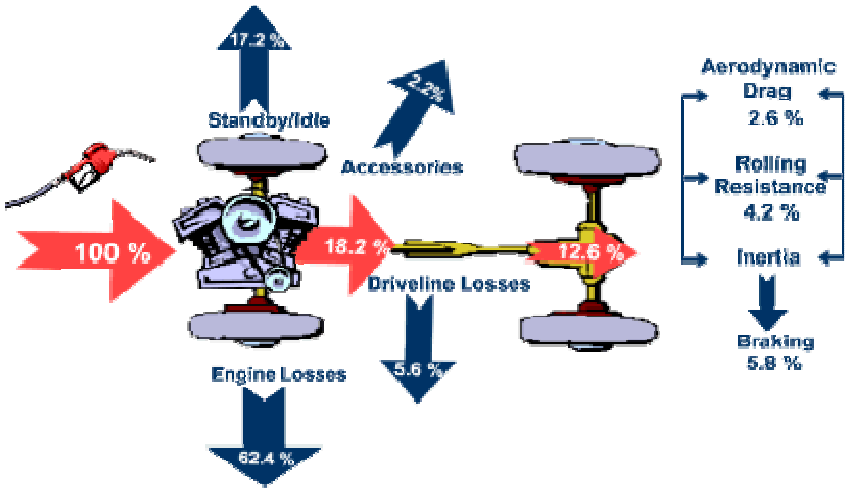

Figure 1. 1 Energy flow of a typical passenger car and the potential energy can be harvested (The energy flow data are sourced from http://www.consumerenergycenter.org/transportation/consumer_tips/vehicle_energy_losses.html)

1.2 Suspension overview

Suspensions play an important role in vehicle's controllability, steering stability and comfort. First, it is well recognized that large vibration will cause discomfort and distract the attention of vehicle operators, which will influence the driving safety. Second, the suspensions are also directly related with the tire-ground contact force and thus affect the steering, mobility, handling, and stability [3, 4]. In addition, recently DOD-supported research [5] indicates that vehicle suspensions have substantial influence on the fuel efficiency.

Figure 1. 2 Different suspension systems with emphases on steering and comfort (The pictures are from: United States Department of Defense gallery and http://blogs.km77.com/arturoandres/514/prueba-de-consumo-7-volkswagen-golf-vi-1-4-tsi-122-cv-dsg/)

The performances of the suspension system are so important that designers want to create some suspension system that can satisfy all the requirements including comfort and dynamic performances. However, passive suspensions have a compromise between passenger ride comfort, handling, and suspension stroke. In addition, the passive suspension will always perform in a pre-determined manner, which cannot be adjusted based on different condition and requirements. So after a long time's development, there are three main different suspension systems including passive, semi-active and active suspension system.

1.2.1 Passive suspension

Passive suspensions are widely used in most of vehicles on road. Their characteristics are predetermined and fixed before manufacturing by the designers based on the potential applications. One of the most important characteristic is the damping for a suspension system. But there is a compromise between comfort and vehicle handling stability. Better comfort can be achieved with a soft suspension, however, the handling stability will be worse. Vice versa. Passive suspension system is most popular for its simplicity, economy and reliability although it cannot achieve best performances according to different requirements.

1.2.2 Active suspension

Active suspension is a smart suspension system which can either dissipate or input energy according to the requirement. Given a control strategy, the active suspension can support the optimal force the vehicle need for optimal performance.

Bose company[6] developed a active suspension system and tested it on a Lexus sedan. It has very good results of vibration isolation and vehicle body control effect.

Despiting the great vibration control performance, the energy consumption of active suspension is huge, which makes it very hard to commercialize.

1.2.3 Semi-active suspension

Semi-active suspension system is a compromise between passive suspension and active suspension. Its damping coefficient can be controlled like active suspension system according to different terrains and different requirements. However, unlike active

suspension system, it can only dissipate energy like passive suspension. As a result, its vibration control ability would be in between passive suspension and active suspension.

Semi-active suspension has already been adopted in some luxury passengers to achieve adjustable, customizable suspension control.

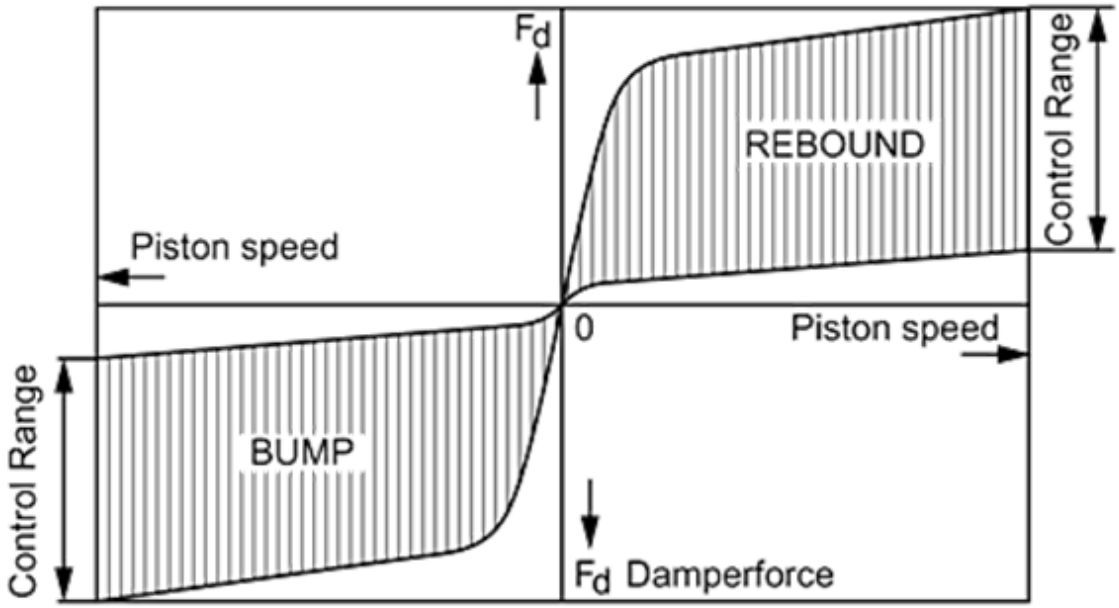

Figure 1. 3 Working range of semi-active damper
(the working range is from http://www.koni.com/121.html)

1.3 Shock absorber overview

The primary function of vehicle suspension is to reduce the vibration disturbance from road roughness, acceleration, deceleration, and cornering to the chassis for better ride comfort and to maintain large tire-ground contact force for better vehicle handling. Traditionally, passive suspension systems consist of springs and viscous shock absorbers. Hydraulic shock absorbers dissipate the vibration energy into waste heat to ensure the ride comfort and road handling. Due to the simplicity and economical market value, passive dampers are favored and used in almost all vehicles nowadays. In order to help vehicles adapt to different terrains and different requirement, semi-active and active suspension systems are designed for the excellence in vibration isolation and vehicle

handling/comfort (Fig 4). However, power consumption and fuel efficiency hit the concern. Regenerative shock absorbers have potential not only to provide sufficient power for semi-active or active suspension control, but also to be used as actuators for semi-active/active control. Besides, it can increase the fuel efficiency by reducing the electrical demand to the car alternator and thus reduce engine's work load.

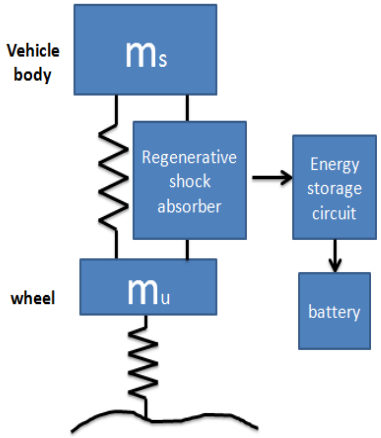

Figure 1. 4 Schematic sketch on the regenerative suspension system

1.4 Regenerative shock absorber design overview

Energy dissipated by shock absorbers are calculated and modeled by a number of researchers. Segel and Lu [7] did some simulation indicating that approximately 200 Watts of power are wasted by four dampers when a passenger car drives on a road at the speed of 30mph. Zuo and Zhang [8] modeled the road roughness and vehicle dynamics, concluding 100-400 watts energy potential from the shock absorbers of a typical vehicle at 60mph.

Over the past 10 years, regenerative braking technology has been highly developed for use in commercialized hybrid vehicles. However, research and development of regenerative suspension systems remains in the primary stage [9].

In 1970s, Karnopp[10,11] first draw people's attention in the power dissipated by vehicle suspensions and power requirement for active suspension system. Velinsky and White[12] analyzed the dissipated power with regard to some factors including vehicle speed, tire pressure and road roughness. Based on that, Segel and Lu[7] did some calculation indicating that 200 Watts of power are dissipated by four shock absorbers of a

passenger car driving on a poor road at 30 mph. Hsu[13] estimated that more than 400 Watts of power can be regenerated from a GM Impact driving at 36 mph. Browne and Hamburg[14] did some experimental research on the energy losses of vehicle suspension. In addition, Zuo and Zhang [8] modeled the road roughness and vehicle dynamics, concluding 100-400 watts energy potential from the shock absorbers of a typical vehicle at 60mph.

Several researchers have explored the concept of regenerative vehicle suspension and there are three main categories including hydraulic regenerative shock absorber, electromagnetic linear motor based regenerative shock absorber and electromagnetic rotary motor based regenerative shock absorber.

1.4.1 Hydraulic regenerative shock absorber(HRSA)

Wendel[15] proposed a regenerative shock absorber based on a hydraulic pump. It can harvest the waste energy in the form of hydraulic power, which could be directly used for hydraulic active suspension system. Fodor and Redfield[16] designed a HRSA system called Variable Linear Transmission to store the vibration energy into a pneumatic accumulator.

1.4.2 Electromagnetic linear motor based regenerative shock absorber

Karnopp[17] proposed the idea of using permanent magnet linear motors as variable mechanical dampers for vehicle suspensions and a new coreless design. Suda et al [18] developed a hybrid suspension system, in which a linear DC generator was used to harvest energy from vibration energy. Goldner et al [19] designed an electromagnetic shock absorber and determined the effectiveness of it based on several experiments. Ebrahimi et al [20] presented the feasibility study of an electromagnetic shock absorber, which could be used as a sensor/actuator. Zuo et al [21] designed a linear electromagnetic energy harvester capable of generating more than 16-64 watts of energy from all four shock absorbers with 0.25-0.50 m/s RMS suspension velocity. This kind of shock absorbers could also be used as force actuators for active control. Martins et al [22] validated the feasibility of electromagnetic active suspensions with some improvement in the areas of power electronics, permanent magnetic materials and microelectronic systems.

1.4.3 Electromagnetic rotary motor based regenerative shock absorber

This approach is to magnify the linear motion with some mechanical mechanisms including ballscrew, rack and pinion and hydraulic transmission. Gupta et al [23] described a comparative study of a linear and a rotary shock absorber. Zhang et al [24] developed a regenerative shock absorber based on ball-screw mechanism and validated the prototype with full-vehicle experiments. Avadhany et al [25] patented one type of regenerative shock absorber based on hydraulic transmission. And Choi et al [26] conbined the controllable electrorheological (ER) shock absorber with a regenerative shock absorber based on rack and pinion mechanism to design a selfpowed controllable suspension. Zhang and Zuo [27,28] developed and tested a retrofittable regenerative shock absorber based on rack and pinion mechanism.

Although the regenerative shock absorbers have been developed for years, the energy density of most designs are still pretty low (figure 1.5). Better designs with higher energy density is necessary for its real application in veihcles.

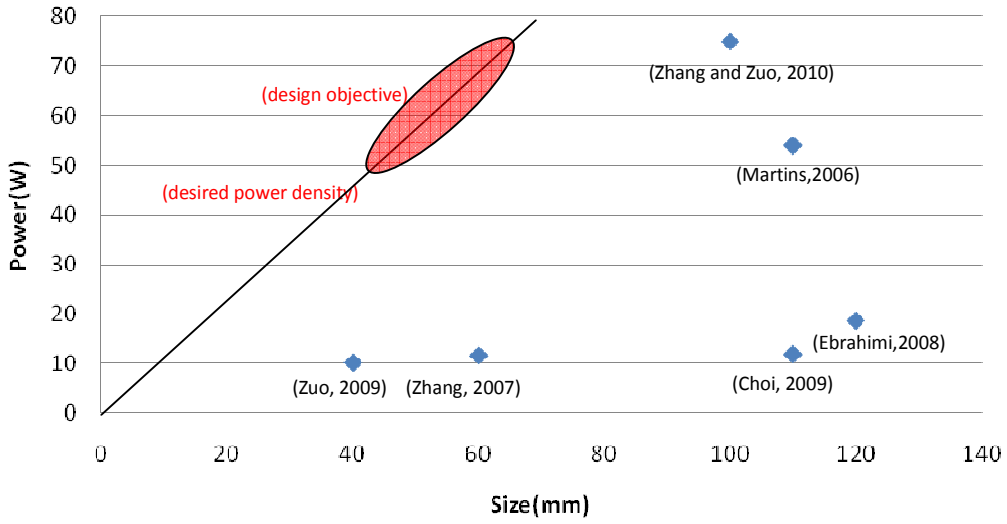

Figure 1. 5 The state of arts regenerative shock absorbers are too large to retrofit into the vehicle suspensions or can't harvest sufficient energy. The data are for 0.2m/s suspension velocity: experiment (square) and simulation (triangle).

1.5 Modeling and control overview

Several regenerative shock absorber prototypes have been developed and tested, but in order to better understand the physical relationships between the dynamic properties and design parameters, dynamic models must be created. Dynamic models will not only give insight to the physical behavior of the prototype but will provide guidance in the improvement of future designs. Several dynamic models for harvesters have been created in the past. For example, Kawamoto et al [29], performed the modeling of a ballscrew based electromagnetic damper for automobile suspension based on differential equations. Cassidy et al [30], took the nonlinear dissipative behavior into consideration and presented the modeling of a ballscrew based eletromagnetic energy harvester for large scale structural vibration applications based on differential equations. Amati et al [31] illustrated the modeling of ballscrew based shock absorbers with differential equations and bond graph methods.

1.6 Regenerative shock absorber design input

We did the experiments on a Chevrolet Surburban (2002 model) to evaluate the suspension's vibration induced by the road roughness. A displacement sensor is directly mounted on its rear shock absorber to measure the relative motion, which is showed in Fig 5. The vehicle is driven on different roads including a local road near Stony Brook and highway (Long Island Express Way I-495).

Figure 1. 6 Experiment setup for suspension vibration tests

Figure 1.6 shows a recorded velocity graph obtained in the test at the vehicle speed of 20 mph. The instant peak to peak velocity can attain 0.15m/s, but the root mean square (RMS) value of the velocity data is only 0.026m/s.

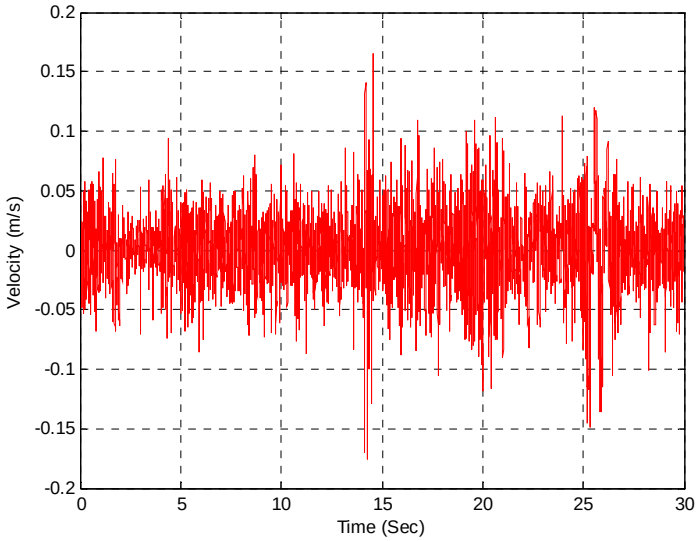

Figure 1. 7 Suspension velocity results on local road at 20 mph

Table 1.1 shows the measured suspension velocities when the SUV was driven at different vehicle speed. From Table 1.1, we can see that the suspension velocity increases when the driving speed increases. Also, the road conditions have great influence on the suspension velocity. Table 1.1 also shows estimated energy dissipated by the suspension system with four shocks.

Table 1. 1 measured suspension vibration velocity and estimated power

Vehicle Speed (mph)	RMS suspension velocity (m/s)	Dissipated power estimation (W)*
20 (local)	0.026	13.5
30 (local)	0.052	54.1
40 (local)	0.084	141.1
55(Highway)	0.077	118.6
60(Highway)	0.090	162.0

*The power is estimated based on four shock absorbers.

1.7 Objective

The objective of the research includes:

Understand the current status of the research on regenerative shock absorbers and explore the way to improve.

Design different types of regenerative shock absorbers with the goal of high efficiency, high compactness and high reliability.

Characterize the prototypes with dynamic models and analyze the performances based on the models.

Test the prototypes with bench tests with strain-stress test machine and road tests for verification and validation.

1.8 Summary

In conclusion, although regenerative shock absorbers have been developed for more than ten years, there are still some problems need to be solved so that this technology could really implemented on vehicles. First, most of the prototypes built by previous researchers are still conceptual designs, there is not much information on how efficient those regenerative shock absorbers can recover energy. Besides, another question should be answered is that if the regenerative shock absorbers act the same as the traditional ones while generating power in real vehicles. This is very important because people don't want to harvest the energy but sacrifice more, like comfort and steering stability. In addition, most of current designs are obviously not retrofit and reliable for vehicle applications. Considering that the working conditions of vehicle shock absorbers are very poor and the space is very limited, regenerative shock absorbers must be designed with rigid restrictions.

1.9 Thesis overview

This thesis consist six chapters, the first chapter gives a general background in vehicle suspensions and different regenerative shock absorbers.

The second chapter described the modeling work and some analysis of the regenerative shock absorber prototype built by Peisheng Zhang.

The third chapter described one improved design of regenerative shock absorber based on motion magnification. This rack-pinion based design is prototyped and then characterized with mathematical models. Road tests are done to validate its feasibility.

The fourth chapter proposed one improved design of the regenerative shock absorber, which introduces one creative mechanical motion rectifier(MMR). Circuit based models are set up in MATLAB/Simulink/Simscape to explore multi-domain dynamics of the system including mechanical structures and electric circuits. The MMR shock absorber is test in lab and on road to verify its advantage over the previous design.

The fifth chapter introduces a new design of MMR regenerative shock absorber based on ball screw. The system is prototyped and analyzed theoretically.

The final chapter presents the summary in the research and recommendations for future work.

Chapter 2 modeling of a rack pinion based regenerative shock absorber

2.1 system description

Figure 2.1 shows the principle of our system. In our design, the housing for the design consists of two cylindrical casings, on which two rod-ends are preplaced to mount to the vehicle chassis and the wheel. The rack and pinion mechanism is used to transform the linear vibration motion of the suspension to rotational motion of a pinion gear. Through bevel gears, the plane of rotation from the pinion gear is redirected and this newly directed motion is transmitted to a gearbox; the gearbox is used to increase rotional speed at that point. Then an electromagnetic motor is used as a generator to harvest electric energy from suspension vibration. The overview of the shock absorber is showed in figure 2.2 and figure 2.3.

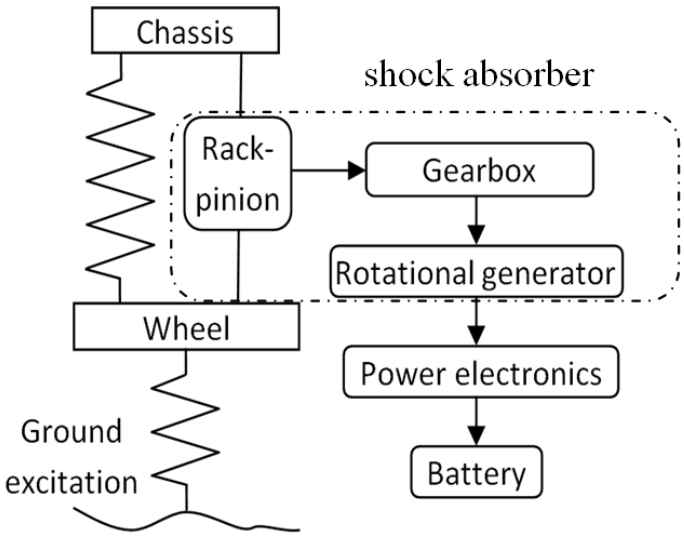

Figure 2. 1 Vehicle suspension system with a regenerative shock absorber

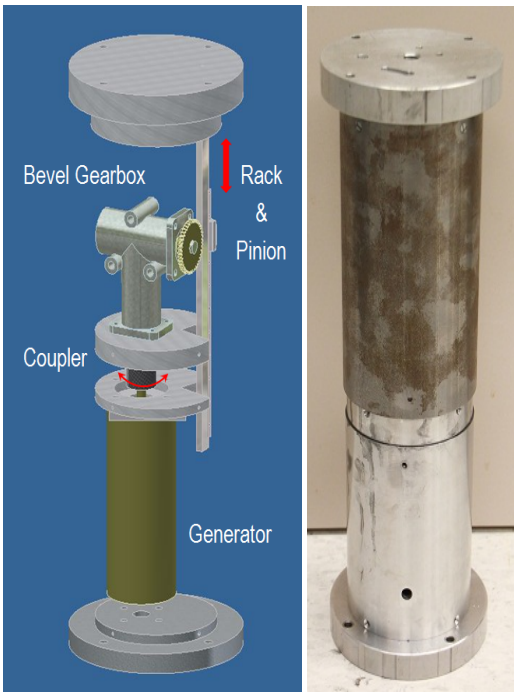

Figure 2. 2 Overview of the rack and pinion shock based absorber [27]

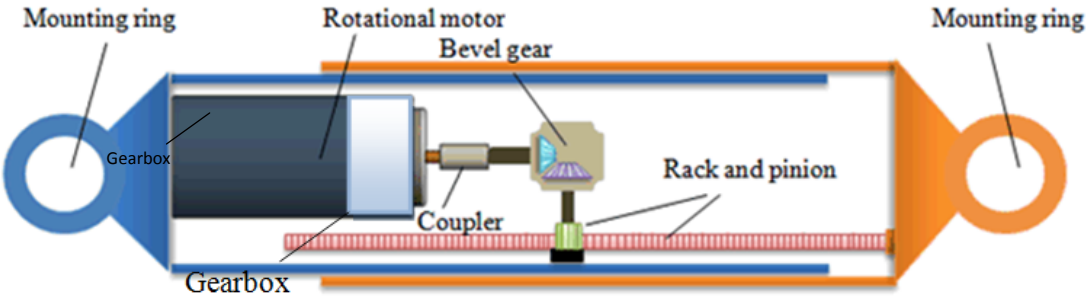

Figure 2. 3 Schematic configuration of the rack and pinion based shock absorber

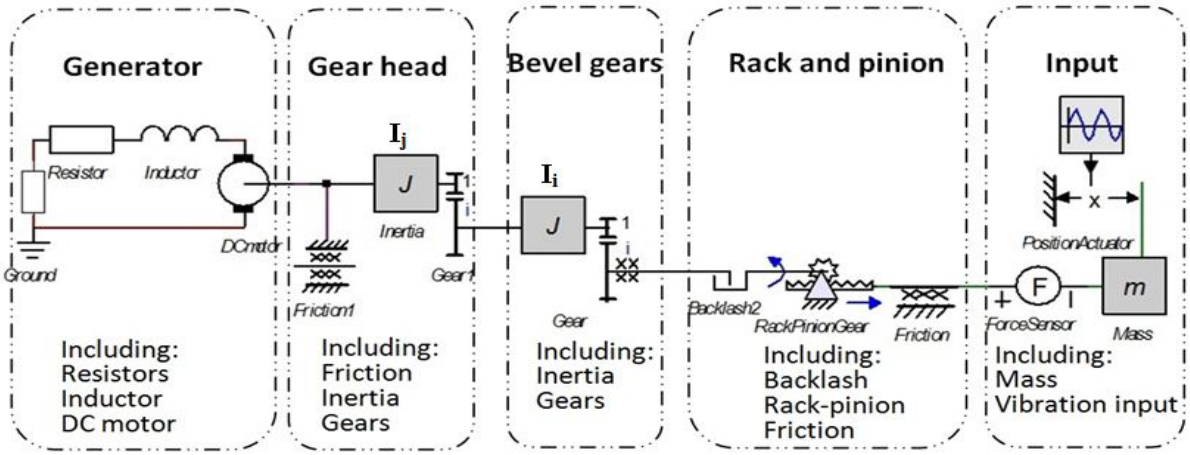

Figure 2. 4 A graphical model for the regenerative shock absorber

2.2 Modeling

The regenerative shock absorber is used to replace viscous damping devices. However, it is more than a damper because of the inertia, backlash and friction of the transmission gears, the resistance and inductance of the generator, and the external electrical load. A complete modelling of the regenerative shock absorber dynamics is necessary to guide our design, evaluate its influence to vehicle dynamics, and implement regenerative semi-active or active control.

The symbol expression for the physical system is drawn in figure 2.4, which models the shock absorber with individual elements. In this section we will first create linear models for each component in the regenrative shock absorber, then model the nolinearity due to friction and backlash, and finally integrate the modelling of the whole regenrative shock absorber system.

2.2.1 Linear modeling

We set the bottom portion (that grounds the generator) as reference and the input excitation is the relative motion of the top portion (rack and casing).

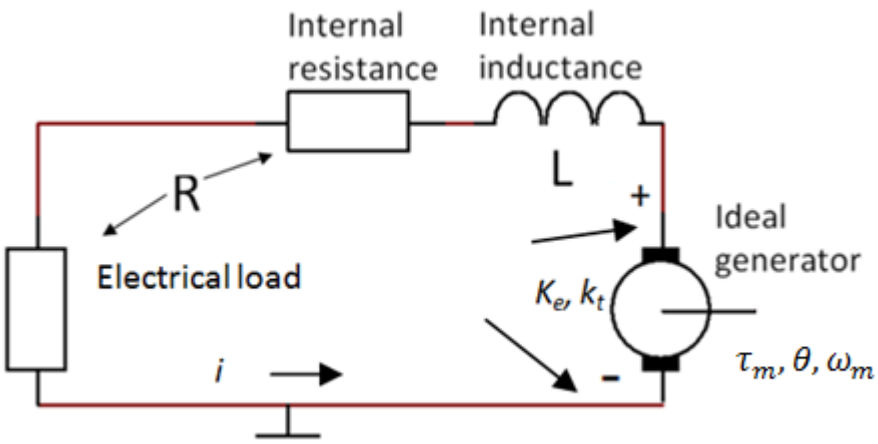

Figure 2. 5 Model of the electromagnetic generator

For the generator (figure 2.5) the rotation will produce a back elecrtromotive voltage V_{ef} propotional to the rotational speed ω .

$$V_{ef} = k_e \frac{d\theta}{dt}$$

where k_e represents the back electromotive voltage constant.

The electric current *i* of the motor will produce a torque $\tau_i$following the relationship:

$$\tau_i = k_t i$$

where k_t represents the torque constant. From the mechanical properties of generators, we can get:

$$\tau_m - \tau_i = J \frac{d^2\theta}{dt^2}$$

where *J*is the inertia of the rotor, and τ_m is the input torque on the motor (generator).

Based on Kirchhoff's voltage laws, we have:

$$V_{ef} - L\frac{di}{dt} - i \cdot R = 0$$

Take all the equations above into consideration, the overall expression of the generator should be:

$$k_e \frac{d\theta}{dt} - \frac{L}{k_t}\frac{d}{dt}\left(\tau_m - J\frac{d^2\theta}{dt^2}\right) - \frac{R}{k_t}\cdot\left(\tau_m - J\frac{d^2\theta}{dt^2}\right) = 0$$

After the laplace transform, this equation could be obtained as:

$$\frac{T}{\Theta} = \frac{k_t \cdot k_e \cdot s}{R + Ls} + Js^2$$

If we express the torque in mass-spring-damping form

$$T = J\cdot\Theta\cdot s^2 + c_m \cdot s \cdot \Theta + k_m \cdot \Theta$$

we could obtain the equivalent damping coefficient(frequency-dependent).

$$c_m = \frac{k_t \cdot k_e \cdot R}{R^2 - L^2 s^2}$$

Also, the equivalent torsional stiffness could be represented in the same way.

$$k_m = -\frac{k_e k_t L s^2}{R^2 - L^2 s^2}$$

As the general road irregularities excitation is between 1-10 Hz and the inductance of the generator (motor) is very small compared with the resistance, the influence of the motor inductance can be neglected. Also, the stiffness effect of the generator is much smaller than the damping effect. Therefore the generator can be simplified as:

$$c_m \approx \frac{k_t \cdot k_e}{R}$$

$$k_m \approx 0$$

The inertia of the motor will be considered together with the transmission as an equivalent mass.

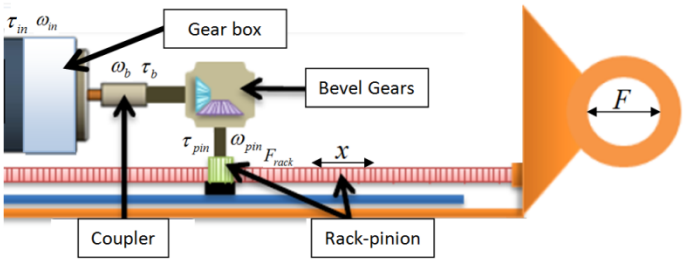

Figure 2. 6 Mechanism of motion transmission

For the gear box of the motor, the input torque of the generator τ_{in} is decreased by k_h and the rotational speed is increased by k_h. The bevel gears have 1:1 transmission ratio. As a result, considering the transmission efficiency, η, we can derive: $\tau_m = \frac{\eta \tau_{pin}}{k_h}$, $\omega_m = \omega_{pin} \cdot k_h$.

The rack and pinion transform linear motion into rotational motion, it follows that $\omega_{pin} = \frac{1}{r} \cdot \frac{dx}{dt}$, $\tau_{pin} = F_1 \cdot r$, where ***r*** is the radius of the pinion, F_1 refers to the force exerted on the rack, and x is the displacement of the rack.

Take x as the variable and based on the Newton's second law, we can determine that:

$$F_1 = \left(\frac{J_G + J_m \cdot k_h^2}{r^2 \eta} \right) \cdot \frac{d^2 x}{dt^2} + \frac{c_m \cdot k_h^2}{r^2 \eta} \cdot \frac{dx}{dt} + f_1$$

where J_G is the total inertia of the pinion gear, the bevel gears, the coupler and their shafts, J_m is the total inertia of the motor rotor $J$and the gearhead, $C_m$is the equivalent rotational damping coefficient of the motor (generator), and f_1 is the friction force.

Then we will consider the rack and pinion to be engaged forming a rigid connection and take the top mass which connects the rack as a steady object to write the differential equation.

$$F - f_2 - F_1 = m_2 \cdot \frac{d^2 x}{dt^2}$$

where $m_2 = (m_r + m_c)$ which includes the mass of the rack and the casing, F is the external force, and f_2 includes the friction force between two outer casing parts and the friction force between rack and its linear guide.

Next, we can derive the force induced by the driving portion:

$$F_2 = (m_r + m_c) \cdot \frac{d^2 x}{dt^2} + f_2$$

In this way, $F = F_1 + F_2$ when the rack and pinion are engaged without backlash.

2.2.2 Friction models

The Stribeck friction model [20] was widely used in situations that include lubricated contact. In this chapter, the Stribeck friction model is adopted to calculate the friction force between the two outer casings, and the friction force between the rack and its plain linear guide (without rollers).

$$f_2 = \left(F_c + (F_s - F_c)e^{-(|\dot{x}_2|/v_s)^q}\right)\cdot \mathrm{sign}(\dot{x}_2) + k_v\dot{x}_2$$

where f_2 is the friction force, F_c the Coulomb sliding friction force, F_s the maximum static friction force, v_s the sliding speed coefficient, k_v the viscous friction coefficient, and q an exponent. The Stribeck friction model is illustrated in figure 2.7.

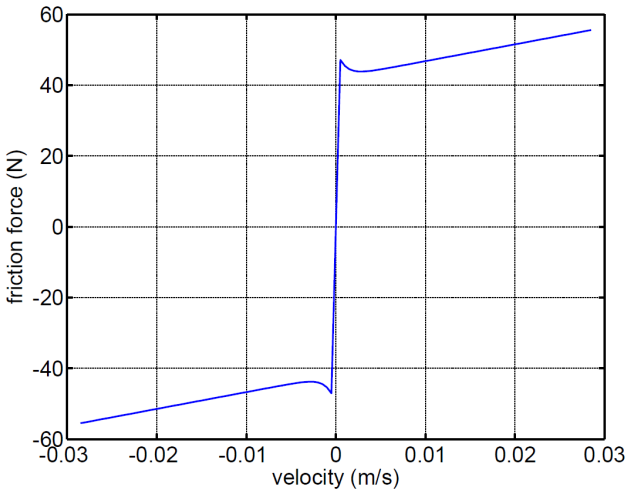

Figure 2. 7 Stribeck friction force model

The friction force in the bevel gears and geared motor is comparably small and can be simply calculated by using the Coulomb friction model:

$$f_1 = f_{10}\cdot \mathrm{sign}(\dot{x}_1)$$

2.2.3 Backlash model

Clearances in the gear transmissions will result in transmission discontinuity and large impact forces. This will influence a system's dynamic properties greatly and must be taken into consideration for the modeling. As the output voltage is proportional to the rotor velocity, the comparison between the shape of output voltage and input velocity can show us the transmission of velocity. It can be seen from figure 2.8 that backlash is the

cause of the discontinuity of the rotor velocity. The integration of the velocity difference (triangular area) equals the backlash dimension [21].

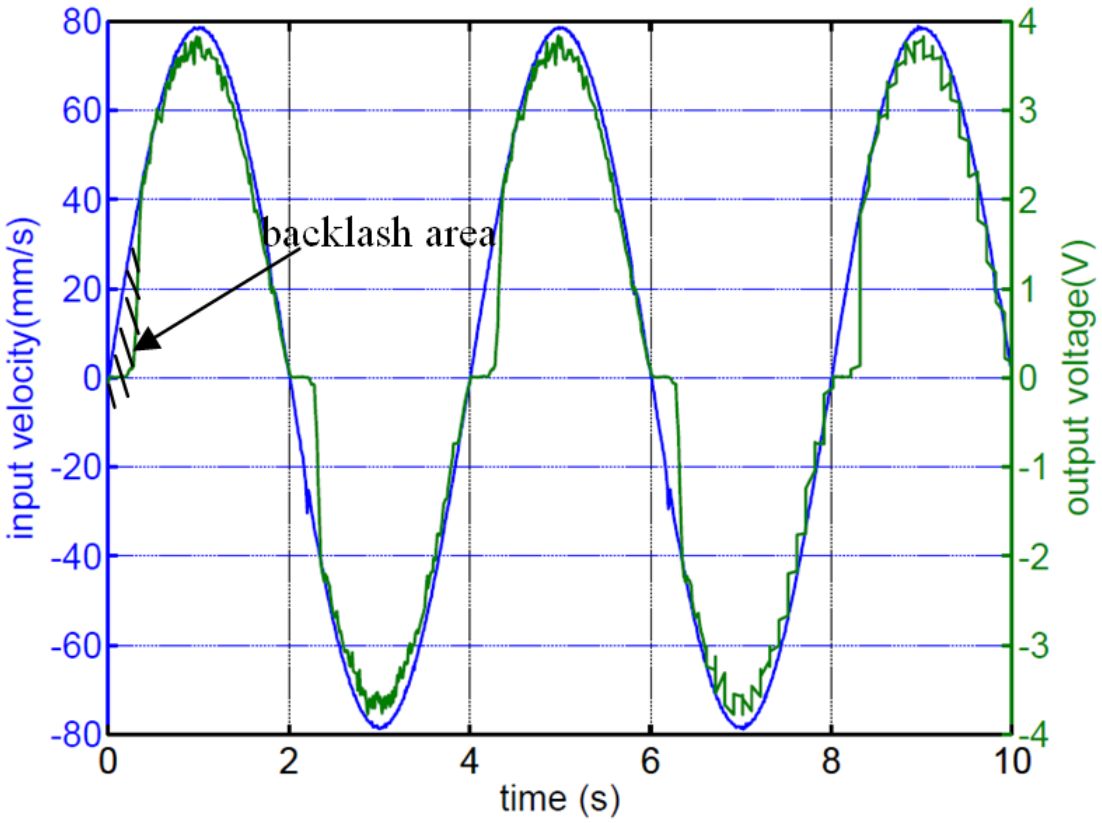

Figure 2. 8 Influences of backlash on motion transmission

Hunt and Crossley [22] developed a method to calculate backlash impact force using a spring-damper model.

$$F_i = K_b \cdot \delta + C_b \dot{\delta}$$

Where $\delta$is the deformation of the teeth when the actual gap goes beyond the static gap B between driving and driven parts, as shown in figure 2.9.

$$\delta = f(x) = \begin{cases} x_1 - x_2 - B & x_1 - x_2 > B \\ x_1 - x_2 + B & x_1 - x_2 < -B \\ 0 & |x_1 - x_2| \le B \end{cases}$$

and x_1 could be calculated via the formulation of the driven part's motion:

$$m_1 \ddot{x}_1 + c_1 \dot{x}_1 + k_1 x_1 = K_b \delta + C_b \dot{\delta}$$

with the initial conditions:

$x_2(0) = x_1(0) \pm B$ ($x_2(0) = x_1(0) - B$ when $x_1>0$; $x_2(0) = x_1(0) + B$ when $x_1<0$)

$\dot{x}_2(0) = 0$

where m_1, c_1, k_1 refer to the equivalent mass, damping coefficient and stiffness of the driven part and x_1, x_2 refer to the displacement of driving part and driven part respectively.

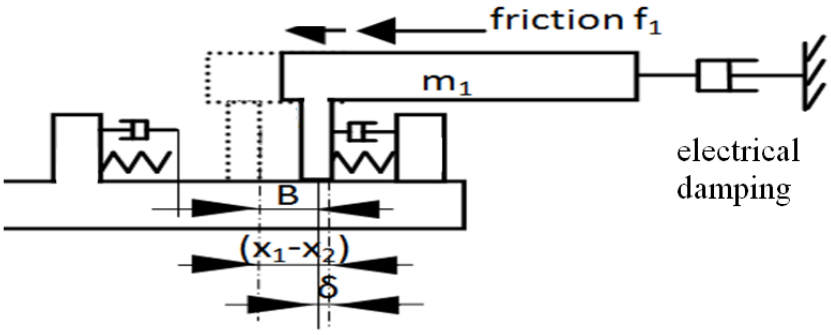

Figure 2. 9 Schematic diagram of spring-damper model of backlash, where the gap is 2B, and the deformation is δ.

Therefore, the force transmitted by the gear could be modeled with a piecewise function:

$$F_G = \begin{cases} 0, & \delta \le 0, \quad \text{no contact} \\ F_i, & 0 < \delta \le B, \quad \text{backlash impact} \\ F_1, & \delta > B, \quad \text{engaged} \end{cases}$$

2.2.4 Overall system modeling

The whole system can be viewed as two primary parts isolated by the backlash in the motion showed in figure 10. The first part will be referred to as the “driving part,” including a mass and a friction force f_1, and a vibration input. For the motion transmissions, backlash influences the dynamic properties seriously. In this system, backlash mainly occurs within the rack and pinion mechanism. It will cause a large impact force and motion discontinuity. The second part is the “driven part,” which includes the bevel gears, planetary gearbox and generator. As a result, this part mostly acts like a damping element with minor inertia and stiffness.

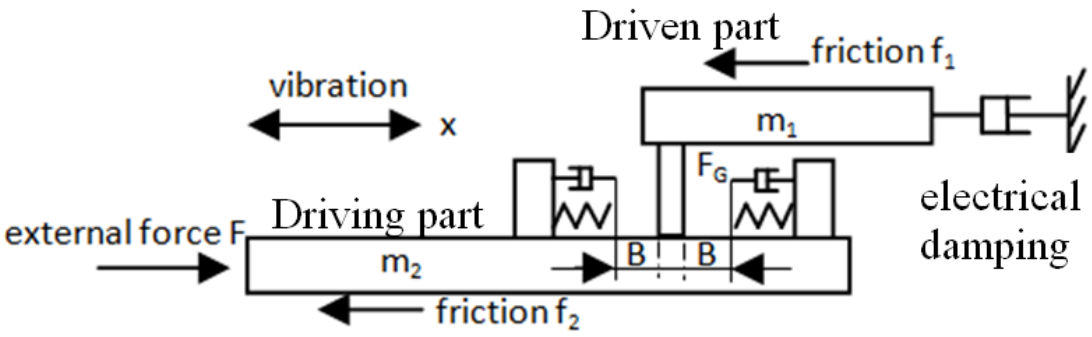

Figure 2. 10 Modeling of the regenerative shock absorber incluidng the motion transmission, generator, backlash, and friction.

According to the three working modes in the backlash, we can obtain the external force piecewise accordingly.

$$F = \begin{cases} F_2 & \delta \le 0, \quad \text{no contact} \\ F_1 + F_2 + F_i, & 0 < \delta \le B, \quad \text{backlash impact} \\ F_1 + F_2 & \delta > B, \quad \text{engaged} \end{cases}$$

Combining the above equations together, we can derive the overal equation.

$$F = \begin{cases} m_2 \cdot \dfrac{d^2x_2}{dt^2} + f_2 \quad , & \delta \le 0 \\ m_1 \dfrac{d^2x_1}{dt^2} + m_2 \dfrac{d^2x_2}{dt^2} + \dfrac{c_m \cdot k_h^2}{r^2 \cdot \eta} \dfrac{dx_1}{dt} + f_1 + f_2 + F_i \, , & 0 < \delta \le B \\ (m_1 + m_2) \dfrac{d^2x_2}{dt^2} + \dfrac{c_m \cdot k_h^2}{r^2 \cdot \eta} \dfrac{dx_2}{dt} + f_1 + f_2 \, , & \delta > B \end{cases}$$

where m_1 and m_2 are the equivalent masses of the driven and driving parts of backlash: $m_1 = \frac{J_G + J_m \cdot k_h^2}{r^2 \eta}$, and $m_2 = m_r + m_c$.

2.2.5 Linear model under sinusoidal vibration

The most dominant case is continuous motion without backlash. Therefore, we analyze the equivalent stiffness and damping coefficient based on the third condition, which corresponding to $\delta > B$.

$$m_{eq} = \left(\frac{J_G + J_m \cdot k_h^2}{r^2 \eta} \right) + \left(m_r + m_c \right)$$

where m_{eq} means the equivalent mass including the rotational inertia of shafts, couplers, bevel gears, pinions and the mass of the rack and the outer casing, J_G η and I_j are defined in equation(7).

From this equation, we can find that the equivalent damping coefficient is mainly determined by the regenerated power and viscous friction.

$$C_{eq} = \frac{k_h^{\,2} \cdot k_t \cdot k_e}{r^2 \cdot \eta \cdot R} + k_v$$

Particularly for sinusoidal vibration input, the inertia component acts like a negative stiffness in the damping loop. For example,

$$x = X \cdot \cos(\omega_0 t + \varphi_0) + x_0$$

$$\frac{d^2 x}{dt^2} = -X \cdot \omega_0^{\,2} \cdot \cos(\omega_0 t + \varphi_0) = -\omega_0^{\,2} \cdot x$$

So the simulated stiffness is negative and it is a “virtual stiffness.”

$$K_{eq} = -\left[\left(\frac{J_G + J_m \cdot k_h^2}{r^2 \eta}\right) + (m_r + m_c)\right] \cdot \omega_0^{\,2}$$

In this way, the whole system can be viewed as a spring element $\boldsymbol{K_{eq}}$ in parallel with a damper $\boldsymbol{C_{eq}}$, which is showed in figure 2.11.

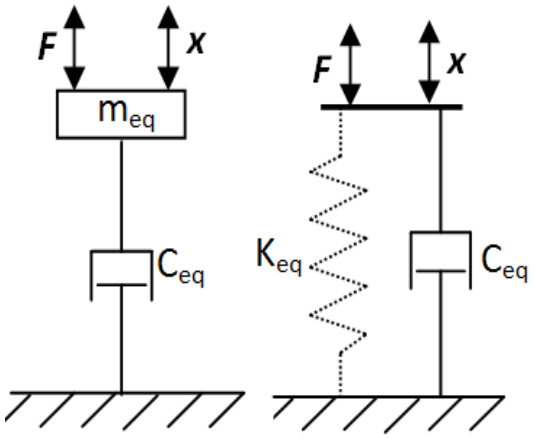

(a) **(b)**

Figure 2. 11 Equivalent dynamic model of the shock absorber: (a) for general input excitation, (b) for harmonic excitation with a negative stiffness

2.3 Experiments and discussions

2.3.1 Experiment setup

The experimental system for the energy harvester is shown in figure 2.12. The experiments were conducted on a 858 Mini Bionix II material testing system from MTS. The vibration energy harvester was mounted on the testing machine and an actuator drove the top portion while the bottom portion was fixed. A dynamic signal analyzer was used to record the voltage signal from the generator. Force and displacement signals were recorded with a displacement sensor and a load cell (integrated in the 858 Mini Bionix II testing system).

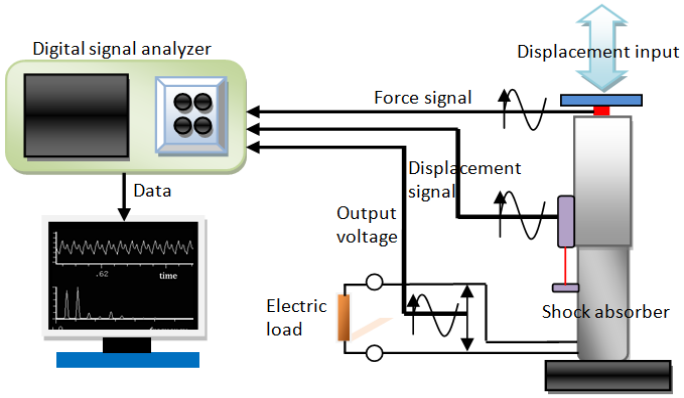

Figure 2. 12 Schematic diagram of experiment setup for the regenerative shock absorber

2.3.2 Parameters

Through direct measurement and indirect estimation, the parameters in the modeling can be obtained. This is showed in Table 2.1, below.

Table 2. 1 Parameters of the regenerative shock absorber

Parameter	*Value*
Mass of the outer casing and the rack(Kg)	3
Back electromotive force constant(V·s/rad)	0.07
Torque constant(N·m/v)	0.055
Motor coil inductance(mH)	1.5
Motor internal resistance (Ohm)	0.8
Transmission ratio of gearhead	9
Radius of pinion(m)	0.0075
External resister connecting generator(Ohm)	1
Equivalent efficiency of gears (%)	85

In the experiments, the excitation magnitude and frequency were 0.1m and 0.25 Hz respectively, and the electric load was 1 Ohm.

By substituting these parameters into the model the features of the energy harvester can be simulated. The final results will be discussed in the following subsection.

2.3.3 Comparison of simulations and experiments

Experimental results are presented in four aspects: 1) Force exerted on the energy harvester; 2) damping loop of the energy harvester; 3) the relationship between the force exerted and velocity and 4) the regenerated electricity.

1) Force

Figure 2.13 shows the simulated and measured forces with sinusoidal vibration input, from which we can see that the model can characterize the main features of the harvester correctly.

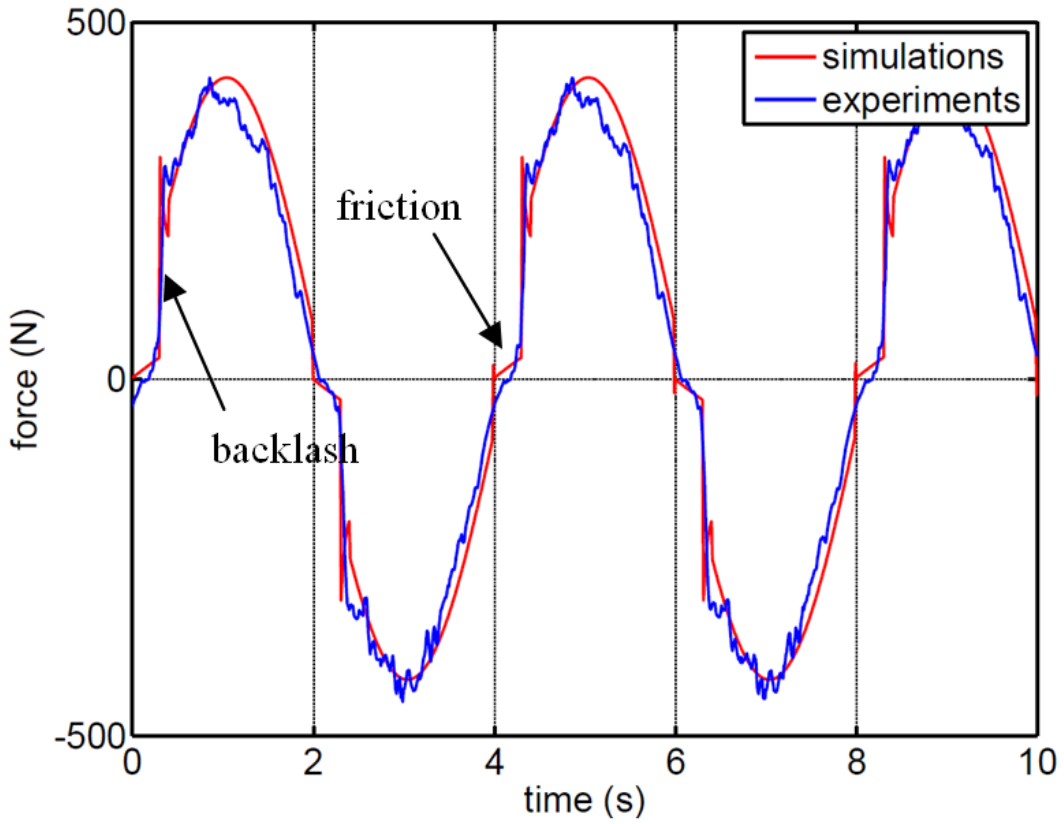

Figure 2. 13 Measured force in comparison with modeling at 0.25Hz sinusoid vibration excitation.

The large force increases are caused by the impacts experienced during backlash reflecting discontinuous transmission.

2) Damping loop

Figure 2.14 shows that the simulated and experimental damping loops.

In this figure, the area of the loop is equivalent to the mechanical work input of the shock absorber, ΔW, for one cycle (roughly 67.14 Nm in experiment). The mechanical power input is $P_{in} = \Delta W \cdot f = 168\,\text{watts}$ And the equivalent damping coefficient:

$$C_{eq} = \frac{\Delta W}{\pi \omega X^2} = 5448\ N \cdot s / m,$$

where ω is the input frequency and $\boldsymbol{X}$ is the displacement magnitude.

It can be found from the modeling that the orientation of the loop is mainly caused by the inertia of moving parts. The orientation represents the equivalent stiffness of the system. In figure 2.13, the slope of the graph orientation is the equivalent stiffness K_{eq}, which is about -619.6 N/m; this is similar to the results from the model (-624.12 N/m).

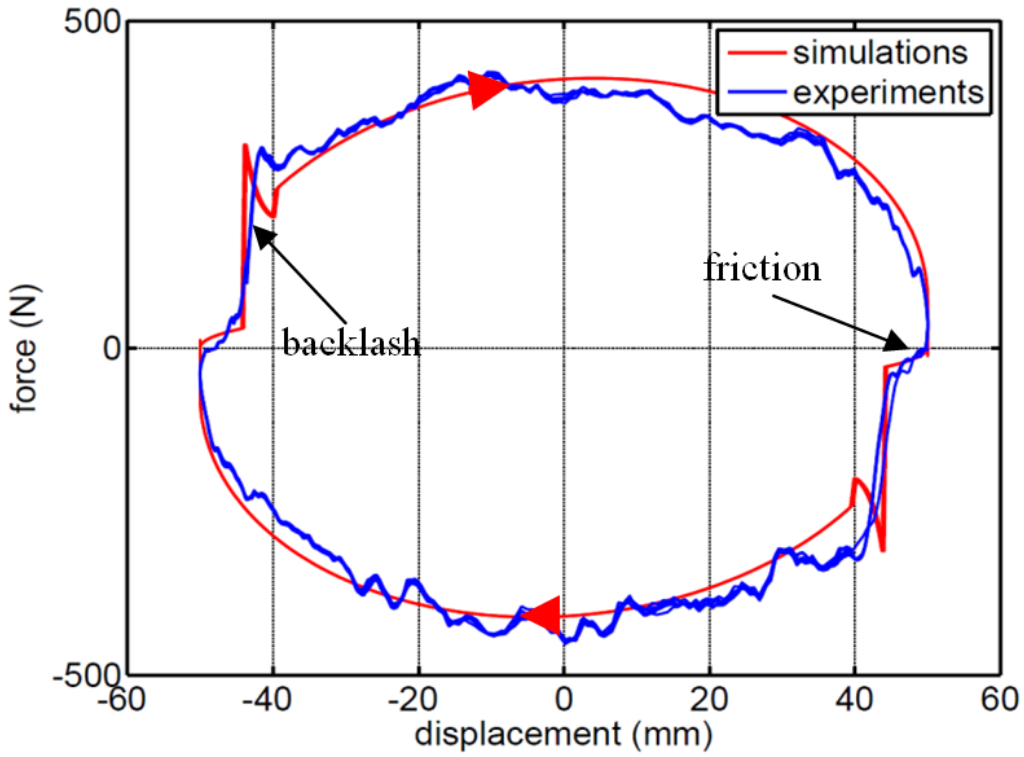

Figure 2. 14 Damping loop force-displacment based on modeling and experiments, where the excitation frequency is 0.25 Hz, and external electrical load is one ohms.

3) Force-velocity loop

The force-velocity loop is shown in figure 2.15. From the force-velocity loop, we can see that slopes are caused by damping and the difference between forward and backward directions is due to stiffness. The hysteresis loop and the sudden force increases are caused by the backlash that occurs in the gear transmission.

From the figure 2.15, we can find that the slope of the curves are close to the results obtained with the models.

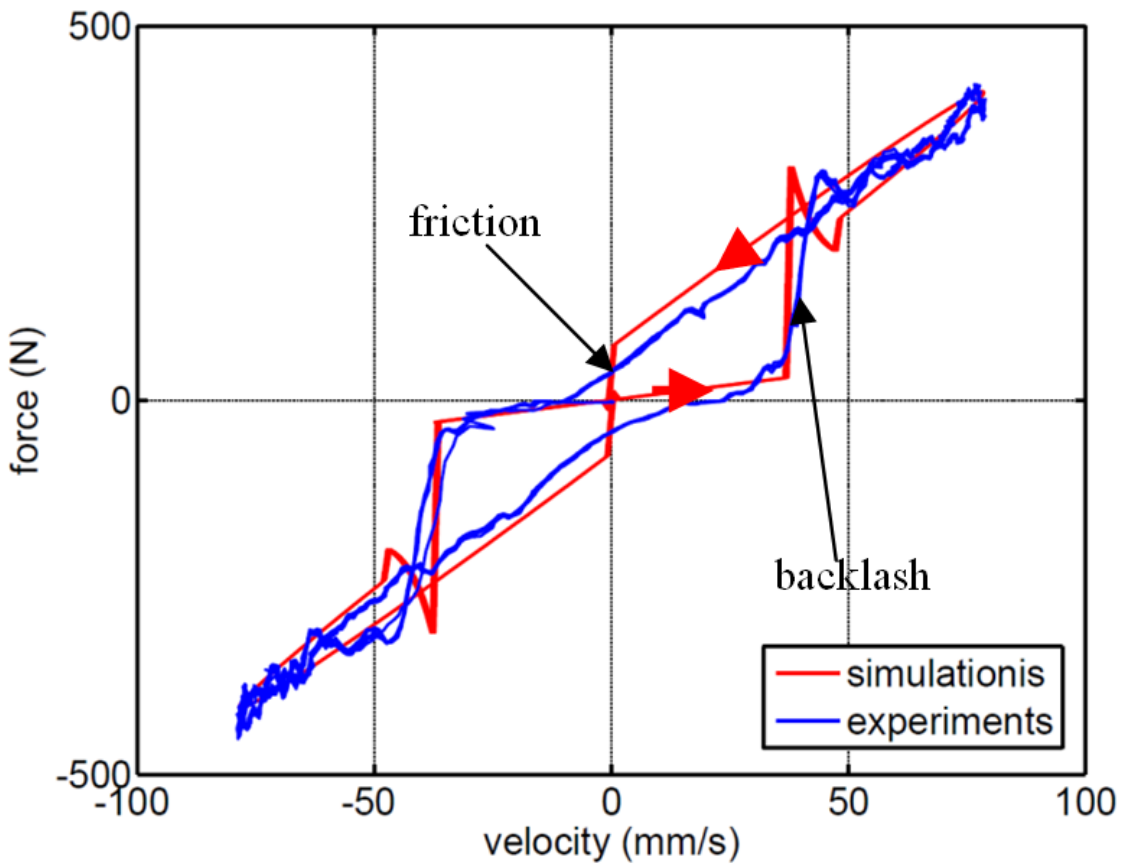

Figure 2. 15 Force-velocity loop based on modeling and experiments.

4) Regenerated electricity

Figure 2.16 shows that the power generation figures obtained through simulation and experiments match well with each other. The average value of output power is 7.3 Watts and the overall efficiency is 44%. This low efficiency is mainly due to the small external load 1Ω (the motor internal reistance is 0.8Ω) and, as a result, the mechanical efficiency can be calculated as 78.2%.

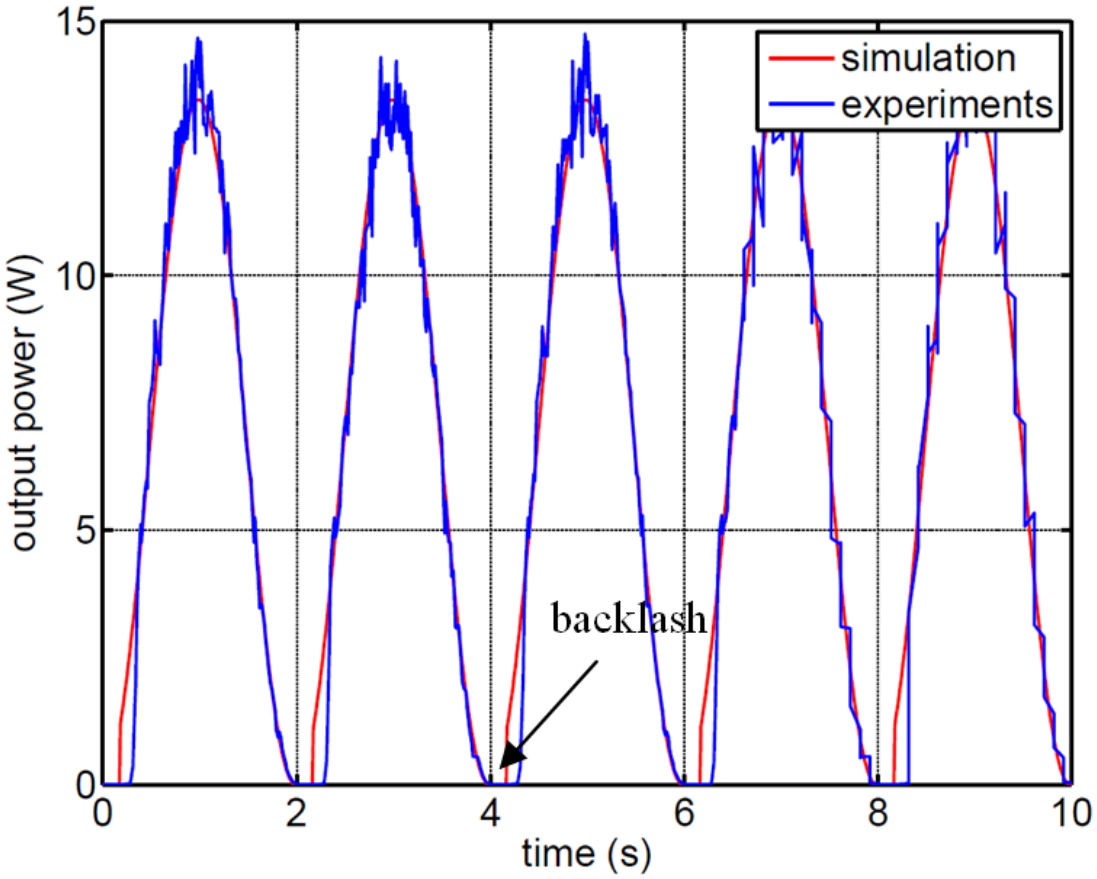

Figure 2. 16 Measured output power on a one ohm resister in comparison with the simulation results (input power=16.78 W)

2.4 Discussions and Conclusions

This chapter showed, by means of an example, a method used for the physical modeling of a regenerative shock absorber based on motion magnification. The example contains rack and pinion gears, bevel gears, a planetary gearbox, and a n electrical generator, in which friction, inertia and backlash were considered. From the results in the analysis, we found that the method of differential equations is fundamental and helps in the understanding of the physical characteristics of the model. The comparison of

experimental and simulated results showed that the two sets match well with each other. Also, physical phenomena of the system such as the “negative stiffness” due to inertia and large force jumps due to backlash under sinusoidal vibration input are explained correctly and precisely by the model.

We can make several comments about how to design an energy harvester with improved performance. We showed that gear backlash significantly influences the dynamic proterties of the system. One suggestion for improvement is to use a roller instead of a simple linear guide for the rack and to add a preload between the rack and pinion. Also, it would be wise to choose more precise gears that experience less backlash. In this chapter, the relationship between the performance index and design parameters are estiblished through modeling, which can be used to further guide the design of retrofittable shock absorber. The dynamic model estibliashed in this chapter for the shock absorber can also be used for semiactive/active control of the suspensions.

The electromagnatic harvester discussed in this chapter can also be used for other large-scale vibration energy harvesting, for example, to harvest the energy and control the vibration of civil structures.

Chapter 3 retrofit design of rack pinion based regenerative shock absorber

3.1 Design introduction

Although the working principle of the previous prototype works well, its size is too large to fit in the current space of shock absorbers. So, a retrofit design with better compactness is necessary for real application on vehicles.

The principle of regenerative shock absorber is shown in Figure 3.1. It is mainly composed of rack-pinion, bevel gears, planetary gears, and an electrical generator. The electric generator assembly is amounted in a cylinder and an outer cylinder is used to enclose the system. The rack is connected with one end of the shock and will drive the pinion when there is some relative motion between the two ends. Through bevel gears, the rotational motion of the pinion gear is transferred by 90 degree to the rotational motion of the generator. The planetary gears are used to magnify the motion and a DC motor is used as a generator.

It should be noted that the authors [12] previously built a rack-pinion based shock absorber prototype, but the shock absorber is not retrofittable for common vehicles, and there are large backlash and friction in the transmission. In order to reduce friction forces and backlash impacts, in this design a roller is used to guide the rack and preload of rack on the opposite side of the pinion gears. In addition, we also put some Teflon ring between the outer and inners cylinders to further reduce friction forces. We also put a filter with steel wire screen at the top of the shock absorber to filter dirt in the air, because the shock absorber works like an air pump and it may suck some dirt into it and break the transmission parts inside. Grease lubrication is also used for gear transmissions.

The bevel gears and rack-pinion gears are two most important components in the system that may cause failure, so the contact fatigue and strength of teeth surface and teeth root bending should be checked [15].

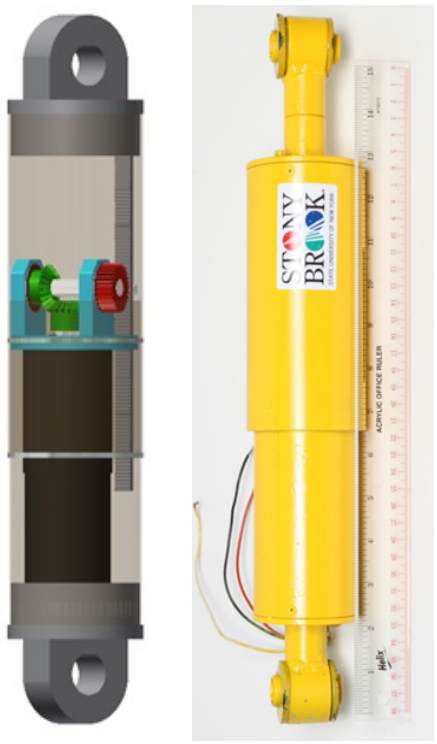

Figure 3. 1 3D model and photo of the shock absorber prototype

3.2 Modeling and Analysis

The regenerative shock absorber has several parts, including generator, planetary gearbox, bevel gears, rack pinion, etc.

3.2.1 DC Motor and DC Generator

Permanent magnetic DC motors can be directly used as generators. However, their characteristics as a generator are totally different from those when it is used as a motor.

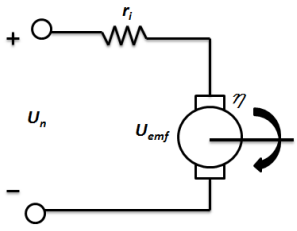

(a)

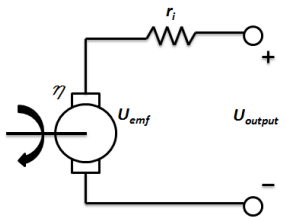

(b)

Figure 3. 2 Two working modes of electrical machines: (a) motor, (b) generator

When the electrical machine is used as a motor, the relation between input voltage U_m and back EMF voltage U_{emf} at nominal rotation speed is

$$U_m = I_n r_i + U_{emf}$$

When it is used as a generator, the output voltage U_g at nominal speed follows

$$U_{emf} = I_n r_i + U_g$$

where the back EMF voltage is proportional to the rotation speed ω_n,

$$U_{emf} = k_e \omega_n$$

where $k_e$represents the back electromotive voltage constant.

So when the motor is used as a generator, at the nominal speed and the nominal current, the output voltage may be much smaller than the nominal voltage of the motor.

$$U_g = U_m - 2 \times I_n r_i$$

And the nominal output power P_g as a generator is also smaller than the nominal power P_m of the motor:

$$P_g = U_g \times I_n = U_m \times I_n - 2 \times I_n^2 r_i = P_m - 2 \times I_n^2 r_i$$

Table 3.1 shows a150W DC motor we selected. Based on Equation 3, we see that the output power at nominal rotational speed and nominal current is 41.1 W. One may think that the output power is maximal when the external resistor is the same as internal resistor. However, a simple calculation indicate the current in the electrical machine will be 2.9A, much larger than the nominal current 1.38A, which is the maximum continuous current the electrical machine can have.

Table 3. 1 Parameters of the 150W DC "motor"

Nominal voltage	Nominal speed ω_n	Nominal current I_n	Internal resistor r_i
48 V	2700 rpm	1.38 A	**6.6 Ω**

3.3 Bench Tests

The experimental system for the energy harvester is shown in figure 3.3. The experiment are conducted on 858 Mini Bionix II material testing system from MTS. A dynamic signal analyzer is used to record the voltage signal from the generator Force and displacement signals are recorded with a displacement sensor and a load cell (integrated in the 858 Mini Bionix II testing system).

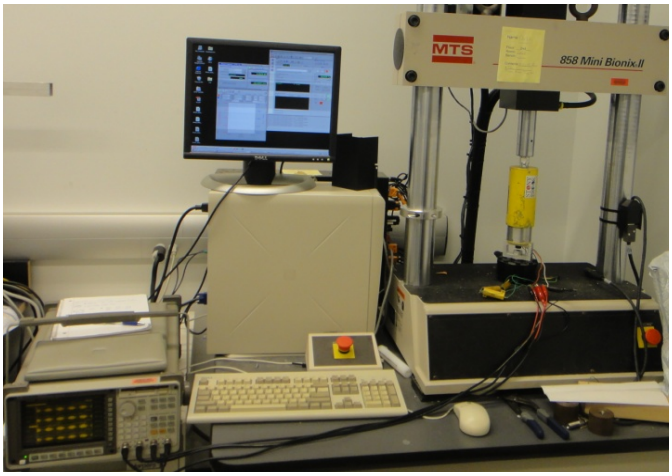

Figure 3. 3 Bench test setup for the regenerative shock absorber

3.3.1 Symmetric test

The prototype was test first with sinusoidal displacement input and a resistive load was used as the electrical load.

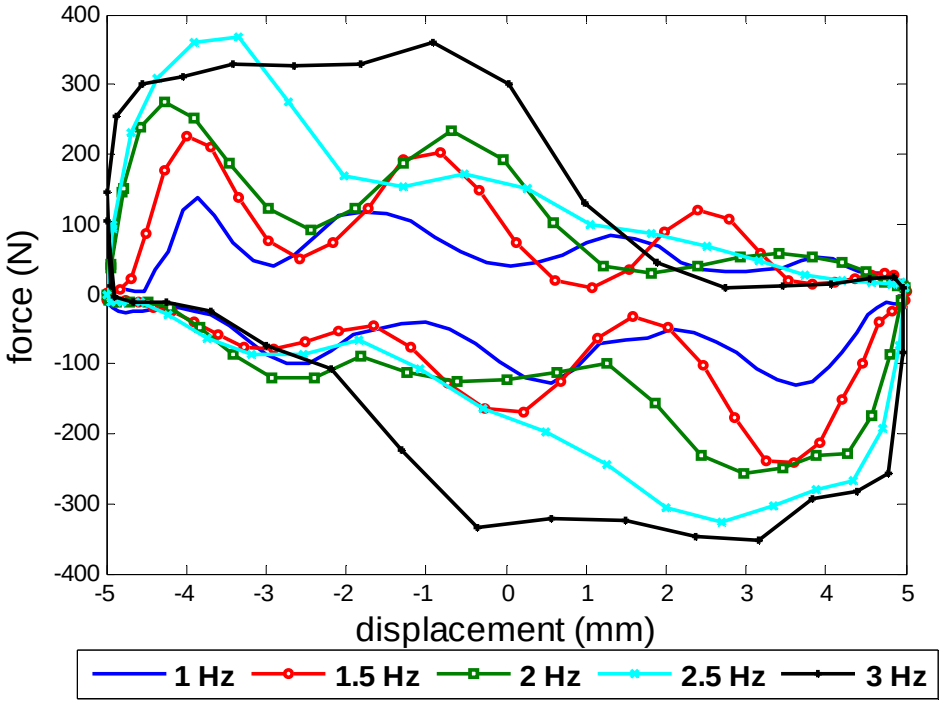

Figure 3. 4 Damping loop for different frequencies with 100 Ohms' external load

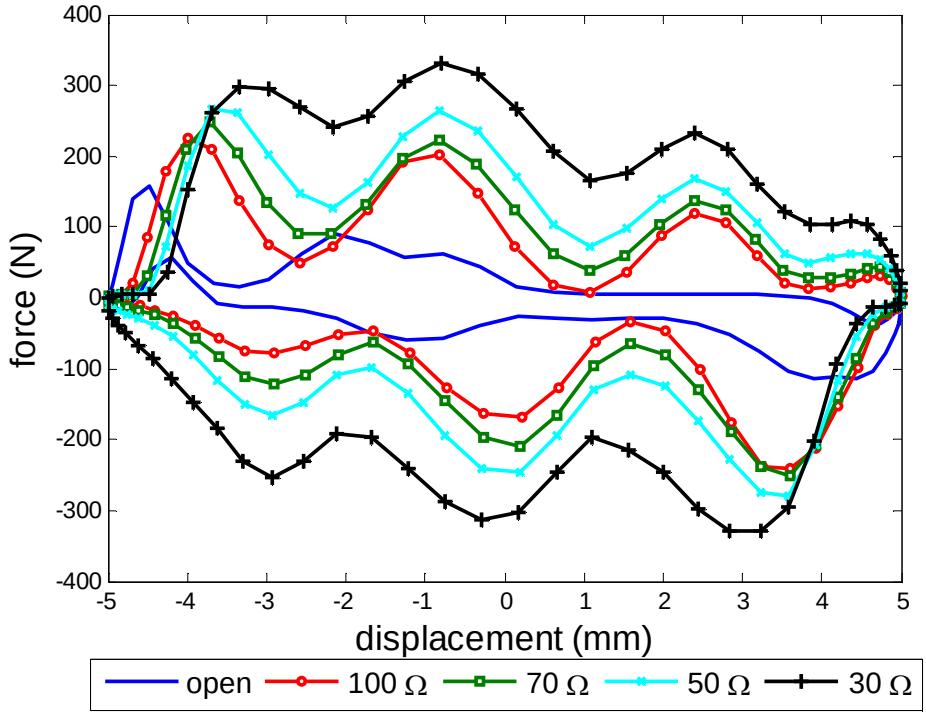

Figure 3. 5 Damping loops for different electrical loads at displacement input of 1.5 Hz's frequency and 10 mm's amplitude.

It can be found that the orientation of the loop is not horizontal and the slope becomes larger when the frequencies increase. From equation (11), we can see that it is mainly caused by the inertia of moving parts and the orientation represents the equivalent stiffness of the system. In figure 3.6, the slope of the graph orientation is the equivalent stiffness K_{eq},

where $K_{eq} = -m_{eq}\omega^2$

In Figure 3.4 & 3.5, the area of the loop means the mechanical work input of the shock absorber ΔW in one cycle, so the mechanical power input $P_{in} = \Delta W \cdot f$. And the equivalent damping coefficient:

$$C_{eq} = \frac{\Delta W}{\pi \omega X^2}$$

where ωmeans the input frequency and $\boldsymbol{X}$ means the displacement magnitude.

Figure 3.6 shows the relationship between force and velocity. We can see that the relationship is almost linear and the slopes correspond to the damping coefficient. In addition, the slopes increase when the electrical load is getting smaller.

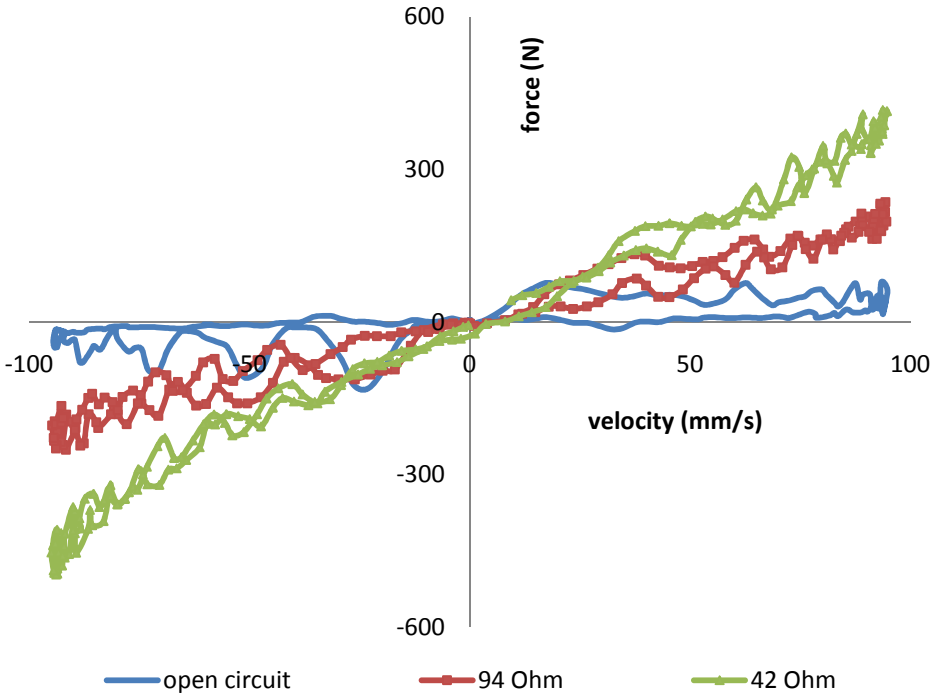

Figure 3. 6 Force-velocity relationship for different electrical loads at displacement input of 0.5 Hz's frequency and 30 mm's amplitude.

We can find from figure 3.7 that the peak output electrical power attains 22 W and 12 W, respectively.

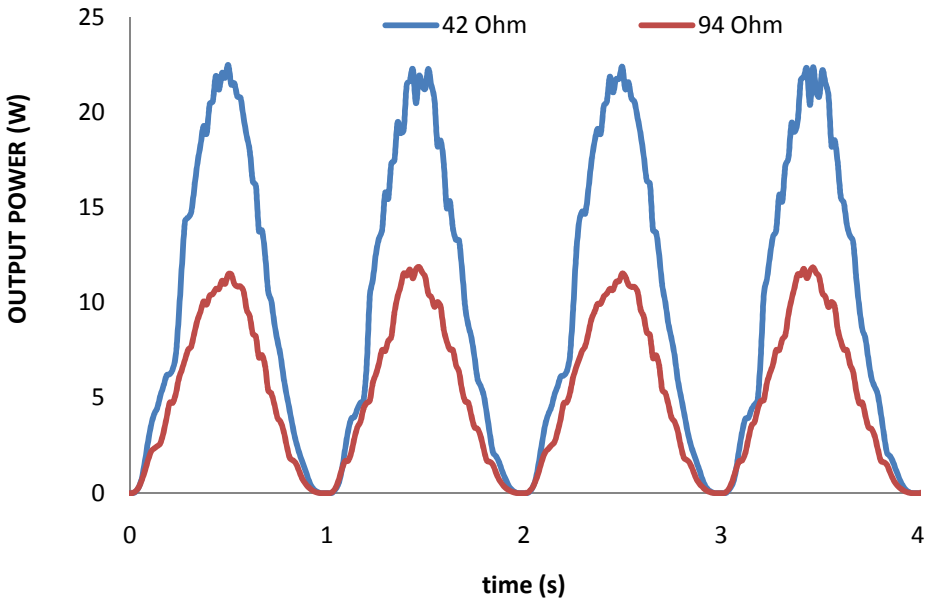

Figure 3. 7 Output electrical power for different resistors at displacement input of 0.5 Hz's frequency and 30 mm's amplitude.

We can use the output electrical power to divide by input mechanical power to calculate efficiency. The mechanical efficiency ranges from 46% to 60% with different frequencies' input and different electrical load. Besides, it can be seen that the mechanical efficiency achieves the maximum around 2 Hz frequency input. In addition, the efficiency gets higher when the electrical load decreases, as showed in figure 3.8 and figure 3.9.

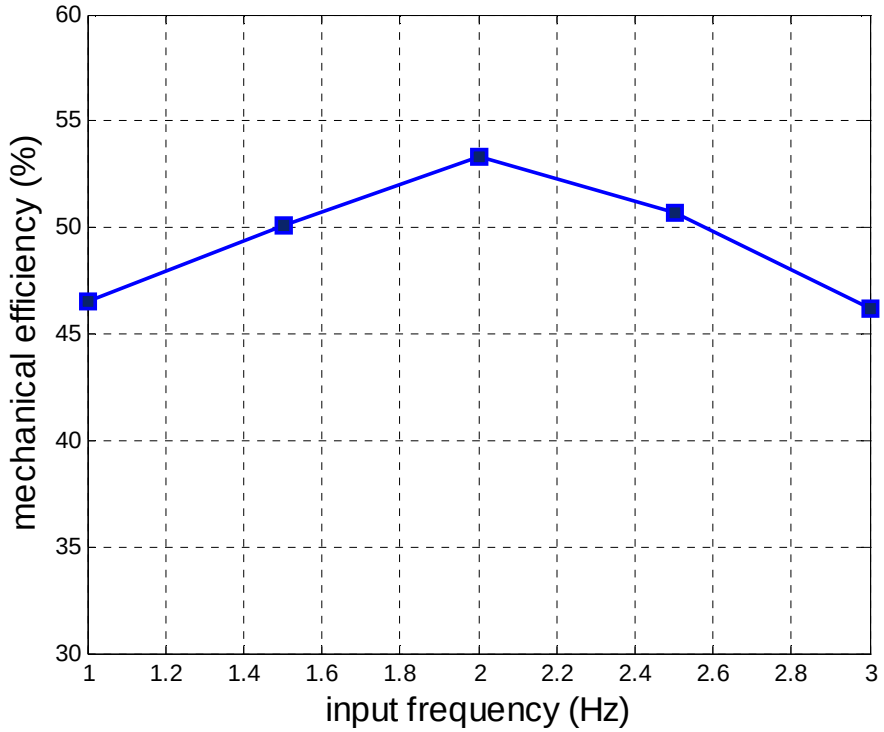

Figure 3. 8 Mechanical efficiency for different input frequencies with 100 Ohm resistive load

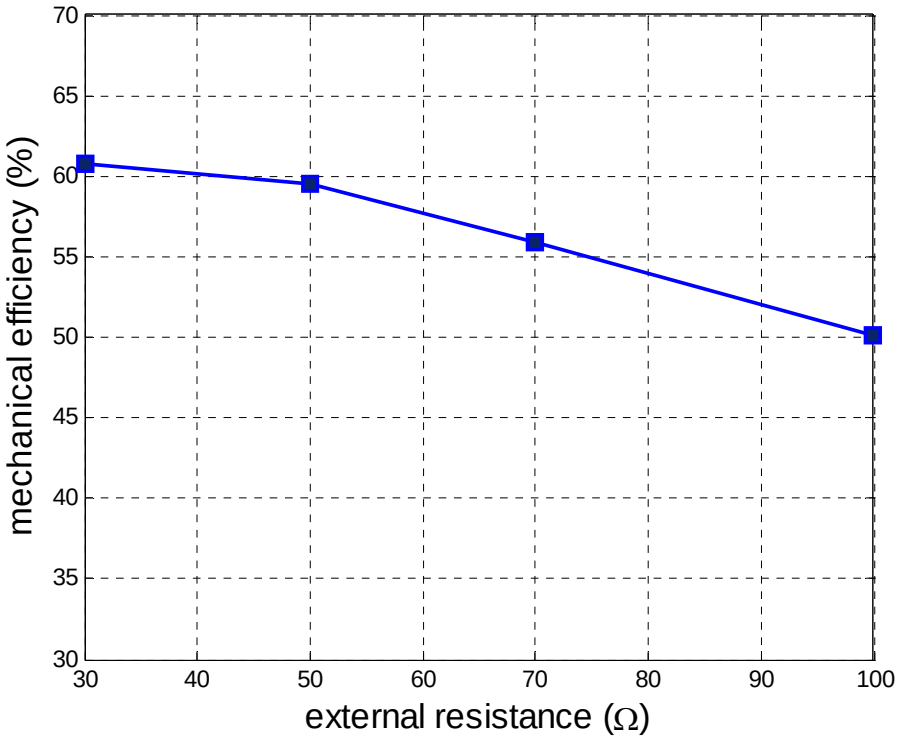

Figure 3. 9 Mechanical efficiency for different external resistance with 0.5 Hz motion input

Equation (10) indicates the damping coefficient of the regenerative shock absorber depends on the electrical loads.

$$C_{eq} = \frac{k_h^2 k_e k_t}{r^2 \eta_g R} + k_v$$

Figure 3.10 shows the damping coefficient's range with different electrical loads. That means the shock absorber can be controlled within the range by controlling the external resistances.

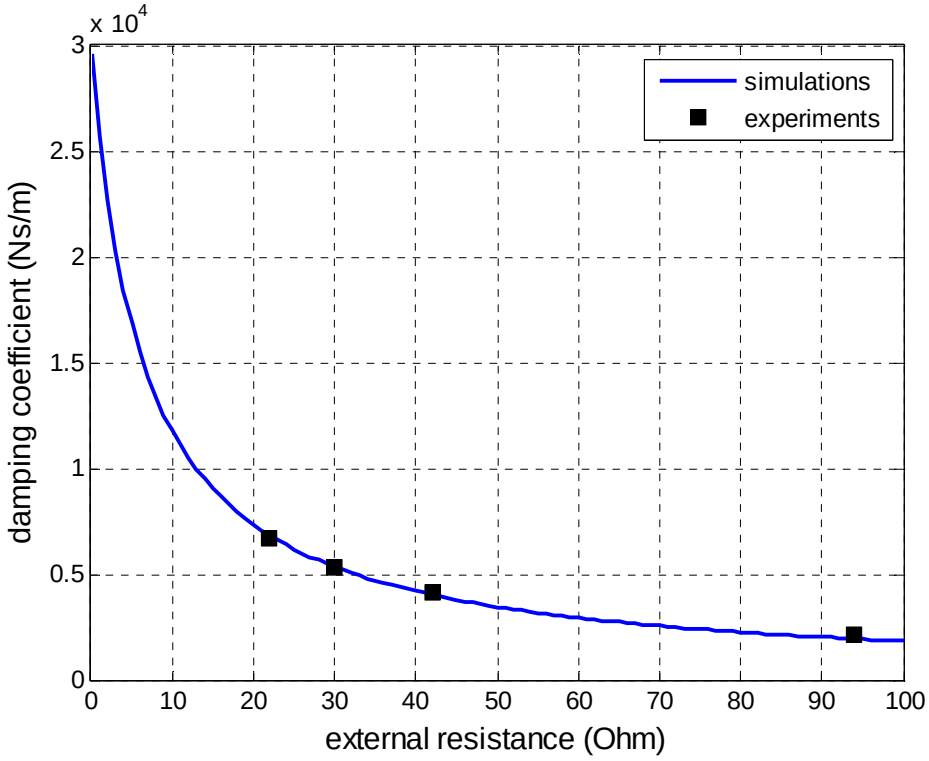

Figure 3. 10 Damping coefficients with different electrical loads

3.3.2 Asymmetric tests

Asymmetric damping coefficients are essential for vehicle suspension system because they can help vehicles keep good contact with roads and reduce the shock to the vehicle body. The regenerative shock absorber is designed symmetrically, however, the asymmetric characteristics can be achieved by shunting the regenerative shock absorber with different electric loads during the jounce and rebound motion. Considering the different motion directions will generate voltages with opposite polarities by the DC generator, a simple circuit can be built to achieve the asymmetry, as showed in figure 3.11.

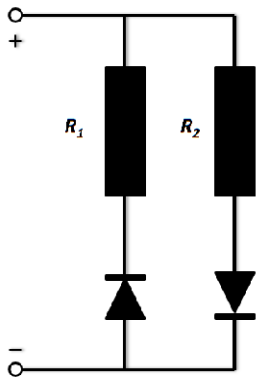

Figure 3. 11 Control circuit for asymmetric characteristics

The circuit showed in figure 3.11 connects R_2in positive direction and R_1in negative direction. So the damping coefficient of the regenerative shock absorber is

$$C_{asym} = \begin{cases} \frac{K^2 k_e k_t}{R_2} & positive\ direction \\ \frac{K^2 k_e k_t}{R_1} & negative\ direction \end{cases}$$

Figure 3.12 & 3.13 show the regenerative shock absorber with asymmetric damping coefficients. We can see that the regenerative shock absorber can act similarly as the traditional hydraulic shock absorber for the asymmetric characteristics. So, the regenerative shock absorber can take place of traditional shock absorbers for its complete function while harvesting energy from the vehicle vibration. In addition, with semi-active/active control law implemented, it can even improve the vehicle dynamics and harvest energy at the same time.

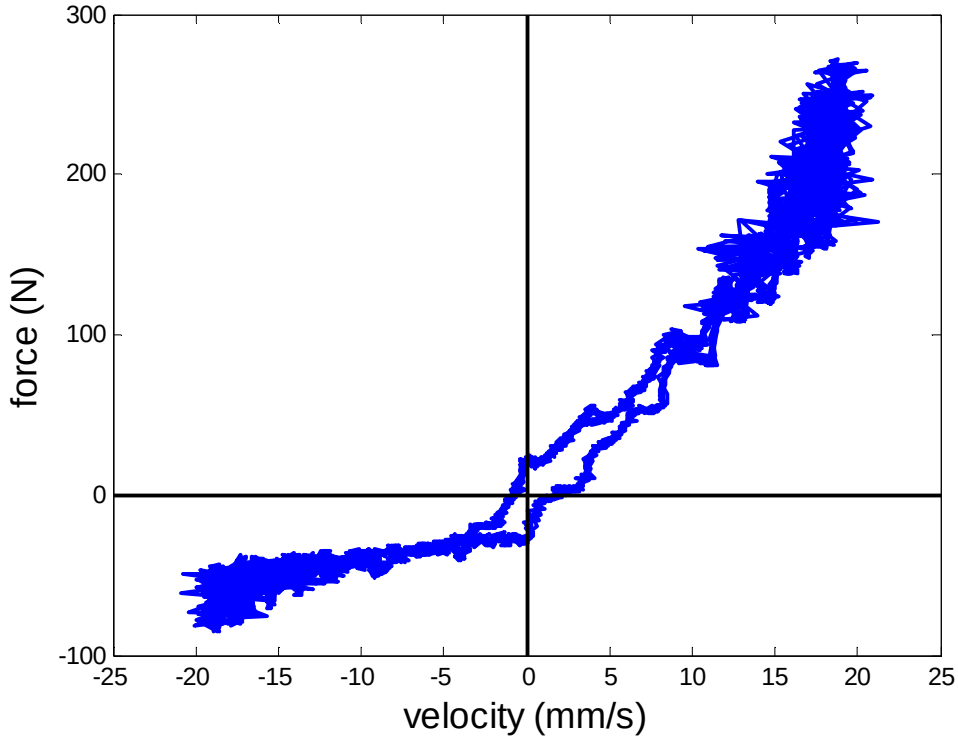

Figure 3. 12 Force-velocity relationship of the regenerative shock absorber

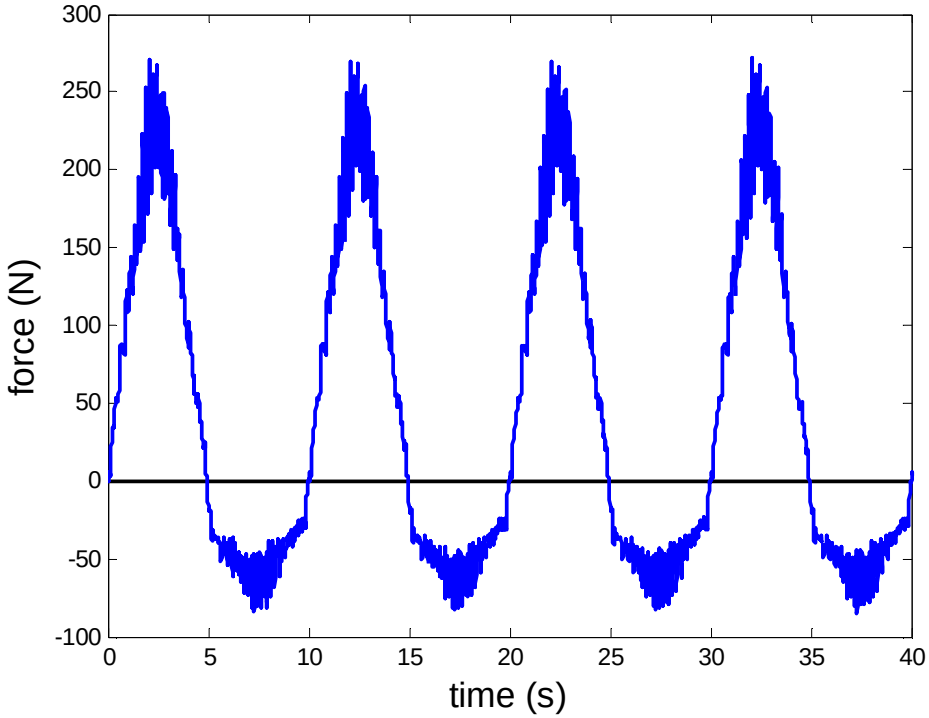

Figure 3. 13 Asymmetric forces of the regenerative shock absorber in jounce and rebound motions.

3.4 Road Tests

In order to validate the theoretical analysis about the energy harvested from the shock absorber and feasibility the prototype, road tests were carried out.

The road tests were done on a Chevrolet Surburban SUV (2002 model). Its information is showed in Table 3.2 [16]. The experiment setup is shown in figure 3.14. The displacement of the rear shock absorber was recorded by a laser displacement sensor from Micro-Epsilon with sampling rate of 1000 points per second. The output voltage is recorded with a HP digital signal analyzer.

Table 3. 2 Vehicle information

Suspension	Suspension type	Diameter (mm)	Curb weight (lbs)
Front	Torsion bar, independent	46	2584
Rear	Multi-link coil, semi-floating	32	2230

Figure 3. 14 Setup of the vehicle, instruments and sensors for road tests

The road tests were conducted on the campus road of Stony Brook University, at different speeds including 20, 30 and 40 mph.

With a 30 Ohm electrical load, the displacement of the vertical vibration of the vehicle and the voltages generated when moving at 30 mph, 20 mph, and 10 mph are shown in figure 3.14, figure 3.15, and figure 3.16, respectively. It can be seen that the peak voltage attains 45 V, 42 V, and 42.8V, respectively. Correspondingly, the peak powers are 67.5 W, 58.2 W, and 61.3 W, respectively. The average power is 4.8 W, 3.3 W, and 1.2 W, respectively, or 19.2W, 13.2W, and 4.8W on four shock absorbers at 30, 20, and 10 mph. Recall in Table 1.1 we estimate 54.1 and 13.5 watts energy dissipation on a local road at 30 and 20 mph. The results from road test are encouraging, though the harvesting efficiency cannot be drawn since the suspension vibration highly depends on the road conditions.

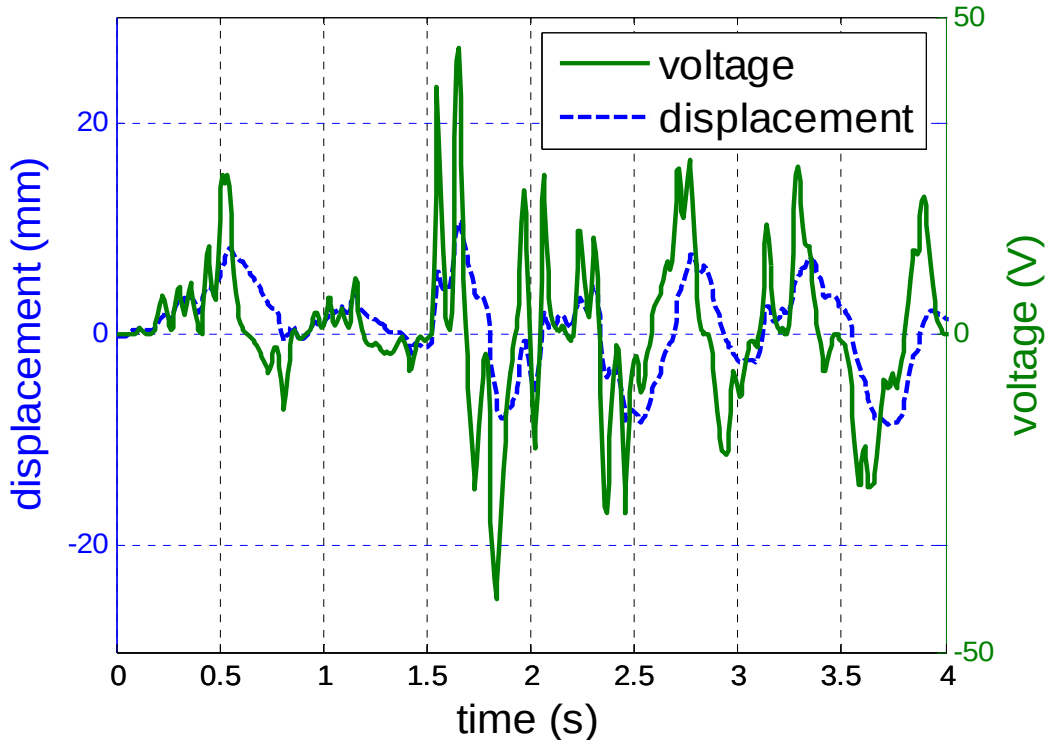

Figure 3. 15 Displacement and voltage measurement at 30 mph on Campus Rd

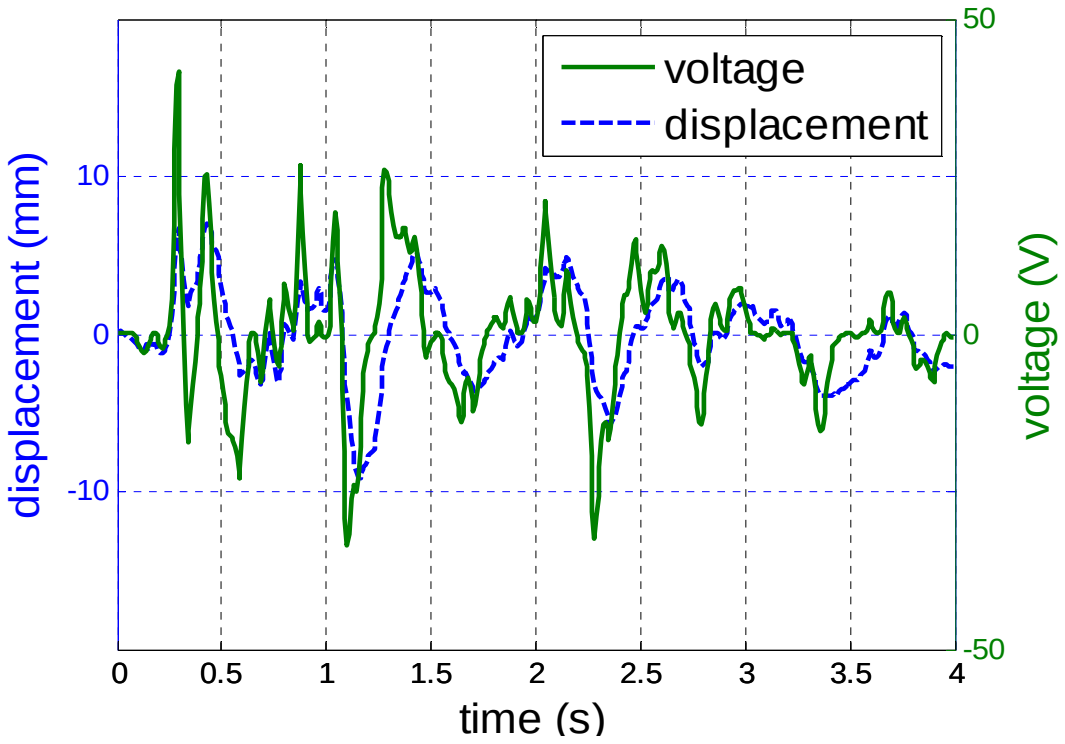

Figure 3. 16 Displacement and voltage measurement at 20 mph on Campus Rd

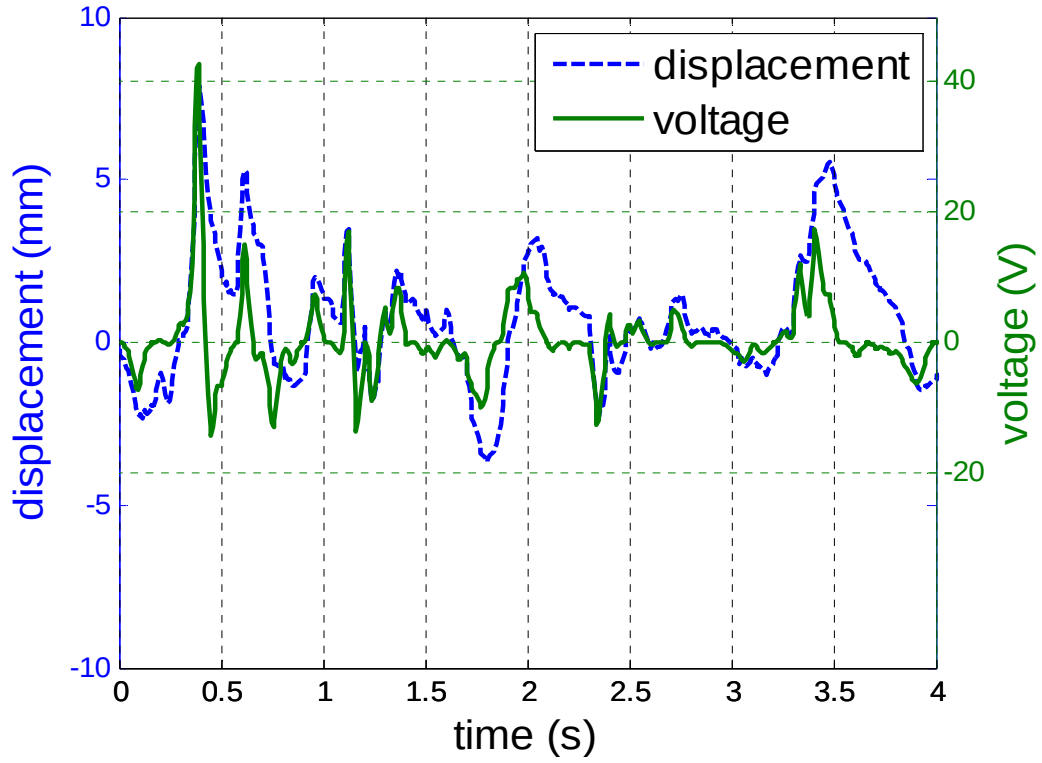

Figure 3. 17 Displacement and voltage measurement at 10 mph on Campus Rd

3.5 Conclusion

A retrofit rack-pinion based electromagnetic regenerative shock absorber is developed and tested which can generate electric power from the road roughness induced suspension vibration of vehicles. The working principle and design are presented. A dynamic model for a rack-pinion type shock absorber system has been derived and analyzed based on differential equations.

The prototype is tested on a testing machine with sinusoidal displacement input. The results show that the equivalent damping coefficient depends on the external electrical resistances. As a result, the regenerative shock absorber can be used as a controllable damper, and the damping coefficient can be controlled by controlling equivalent external electrical load. A total energy conversion efficiency of 56% is achieved. The regenerative shock absorber could also attain asymmetric performances in jounce and rebound by connecting it with asymmetric load circuits.

Road tests were also carried out to verify the performance of the new designed regenerative shock absorber. The experiment results indicate that the generated voltage reflects the road irregularities well. A peak power 270 watts and average power 20 watts can be obtained from four energy-harvesting shock absorbers when the vehicle travels at 30mph on campus road.

Chapter 4 Rack pinion based regenerative shock absorber with mechanical motion rectifier

The rotary energy harvesting absorbers translate the up-and-down suspension vibration into the bi-directional oscillation of the electrical generation and produce electricity. Since low-cost and off-shelf rotary generator can be used, they are more compact and cost effective. However, the irregular oscillation of the motion mechanism causes numerous problems such as low mechanical reliability and bad vibration performance. For example, the ball screw mechanisms investigated in [19-22] have a good power density, but the absorber is too stiff to control at high frequency due to large motion inertia, resulting worse ride comfort at high frequency above 7-10 Hz even with active control [23,24]. More important, the bidirectional oscillation will cause large impact force, backlash, and friction in the transmission system, causing the fatigue or even failure. The rack teeth were worn out and broken quickly due to large impact force in our early prototype of regenerative shock absorber based on oscillatory rotation generator. In addition, the bidirectional oscillating motion will produce an irregular AC voltage. In order to charge batteries or power vehicle electronics, the voltage needs to be commutated with electrical rectifier, in which the forward voltage of diodes unavoidably reduces the circuit's efficiency.

The main contribution of this chapter is an innovative concept of "mechanical motion rectifier", which can convert bidirectional motion into unidirectional motion. It is not a substitute of electrical voltage rectifier. It can significantly improve the reliability by reducing impact forces and increase efficiency by decreasing the influences of friction. It also enables the electrical generator to rotate unidirectionally at relative steady speed with higher energy efficiency. The second contribution is a circuit based modeling to analyze the system's dynamic properties both in electrical domain and mechanical domains. The third contribution of this chapter is simulation and lab experiments to verify the concept and advantages of mechanical motion rectifier based vibration energy harvester.

4.1 Principle of Motion Rectifier

Shock absorbers are installed between chassis and wheels to suppress the vibration, mainly induced by road roughness, to ensure ride comfort and road handling. Conventional rotational regenerative shock absorbers translate the suspension oscillatory vibration into bidirectional rotation, using a mechanism like ball screw or rack pinion gears. Figure 4.1 shows one such an implementation [25], where the rotary motion is changed by 90 degree with a pair of bevel gears for retrofit.

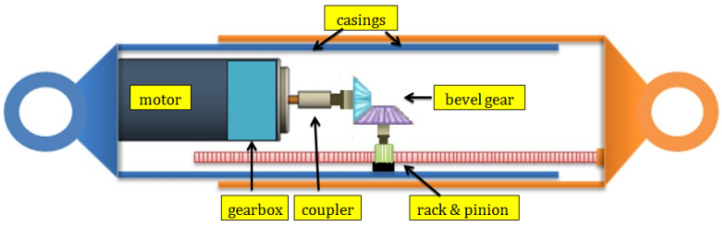

Figure 4. 1 Traditional design of a rack-pinion based regenerative shock absorber [25]

A "motion rectifier" is created to "commutate" oscillatory motion. Its principle is showed in Figure 4.2. We can define the functioning of the "motion rectifier" with two working modes: positive mode and negative mode. The key components of "motion rectifier" are two roller clutches that transmit rotation only in one direction and dive the motion in two different routes. As a result, the shaft of the motor and planetary gear will move always in one direction.

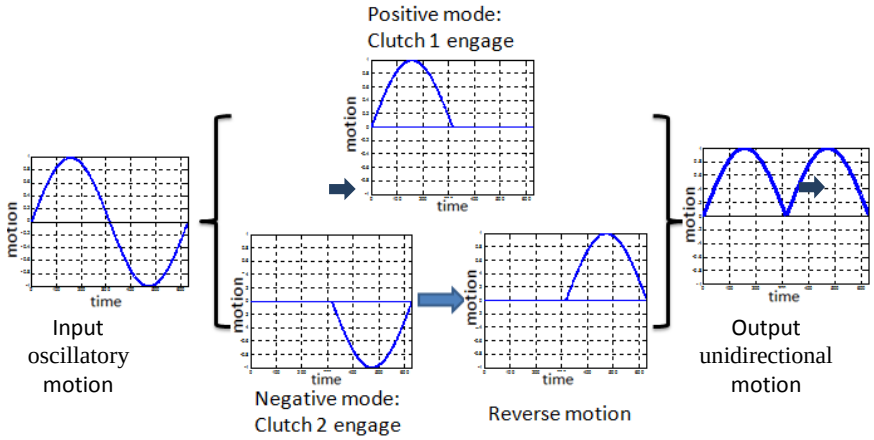

Figure 4. 2 Principle of "motion rectifier" for oscillating motion

The mechanical motion rectifier with two roller clutches can be analogy to a full-wave voltage rectifier using a center-tapped transformer and two diodes, as shown in Figure 4.3. It converts the irregular reciprocating vibration into the regular unidirectional rotation. And the system inertia is equivalent to the electrical smoothing capacitor in series with the electrical load.

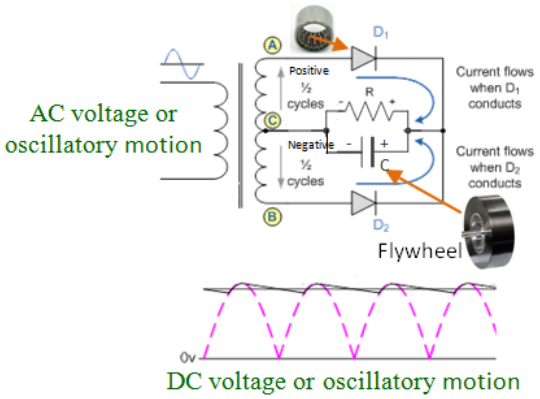

Figure 4. 3 Electrical analogy for "motion rectifier"

4.2 Design of Highly-Compact Motion Rectifier Based Harvester

A convenient design of the "mechanical motion rectifier" that directly translates the above "center-tapped transformer" into the mechanical domain may involve one input like double-side rack as the primary coil and two outputs like two pinion gears as two secondary coils, as in [26]. However, it needs 2-3 shafts and the overall size is too large for retrofit application of suspension. Moreover, overall efficiency is comparatively low considering every engagement like gear transmission or shaft typically has an efficiency of about 90%.

In order to keep regenerative shock absorbers compact enough, the motion transmission needs to be well organized to fit into the existing space of the shock absorber. In additional, we should decrease the number of gear pairs and shafts to improve the mechanical efficiency. Figure 4.4 shows the new design we proposed. In this design we use a pair of rack and pinion, one shaft and three bevel gears. Two roller clutches (blue) are mounted between the shaft (gray) and the two larger bevel gears (purple), which are always engaged with the small bevel gear (green). The different size of bevel gears will give additional transmission ratio; they can be of the same size if additional transmission ratio I not needed.

When the rack moves up and down, the pinion and shaft rotate clockwise and counterclockwise directions. Due to the engagement of the one-way roller clutches, at an instant time only one large bevel gear will be engaged and be driven by the shaft; another large bevel gear will be disengaged from the shaft by the roller clutch. These two larger bevel gears will be driven in opposite direction by the shaft. Since the large bevel gears are in two opposite sides of the small bevel gears, the smaller bevel gear (and the generator) coupled to it will always be driven by either left or right bevel gears and will rotate in one direction no matter the rack goes up or down.

The assembly of the pinion, shaft, and bevel gears will be mounted to one cylinder, and another cylinder covers outside and to guide the linear motion. Similar as roller bearings, the roller clutches can't hold large thrust in the axial direction, so two thrust bearings are designed to support the thrust forces on the two larger bevel gears. In order to reduce the friction between the inner and outer cylinders, we insert Teflon rings between the two cylinders. The rack is preloaded and guided by a roller in the place opposite to the pinion. The enclosed construction of the shock absorber prevents dirt from hurting gears inside.

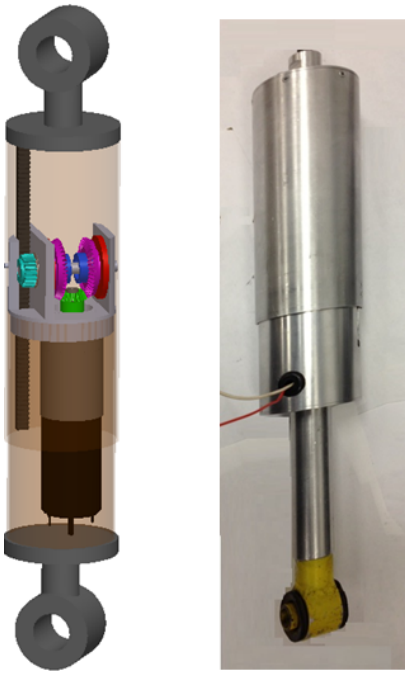

(a)

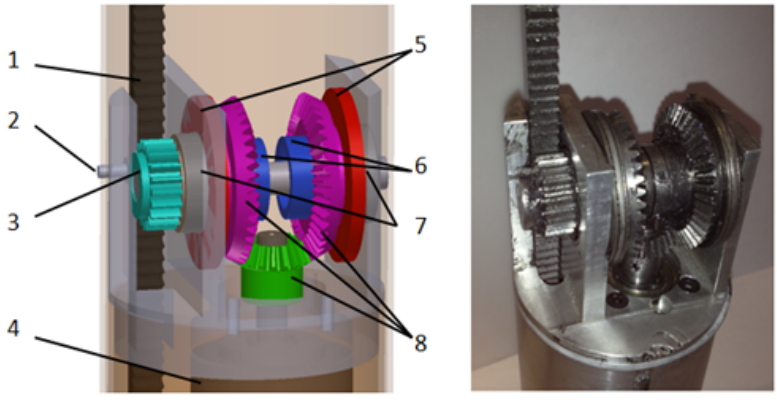

1 rack
2 roller
3 pinion
4 planetary gears and motor
5 thrust bearings
6 roller clutches
7 ball bearings
8 bevel gears

(b)

Figure 4. 4 Comparison between 3D model and actual prototype, (a) overall view, (b) inner structure

4.3 Modeling And Simulations

4.3.1 System analysis

The energy-harvesting shock absorber is used to generate power from the vibration of vehicle suspension. Such a shock absorber itself is a dynamic system which includes generator, transmission gears, motion rectifier, etc, as shown in Figure 4.5. A dynamic modeling is necessary to guide the design and power management to achieve the

maximum power harvesting efficiency. In this section, we will first analyze the parts with differential equations and then introduce the modeling of the overall system with an innovative modeling method based on the circuits.

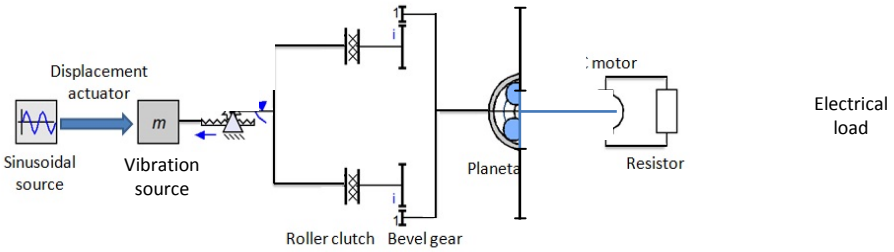

Figure 4. 5 Simplified schematic view of the motion rectifier based energy-harvesting shock absorber

For the DC generator (figure 4.6) in our system, rotational motion will produce a back electromotive voltage V_{ef} proportional to the rotational speed ω.

$$V_{ef} = k_e \frac{d\theta}{dt}$$

where k_e represents the back electromotive voltage constant.

The electric current i of the motor will produce a torque $\tau_e$following the relationship:

$$\tau_e = k_t i$$

where k_t represents the torque constant. From the mechanical properties of generators, we can get:

$$\tau_m - \tau_e = J_m \frac{d^2\theta}{dt^2}$$

where J_m is the inertia of the rotor, and τ_m is the input mechanical torque on the generator.

Based on Kirchhoff's voltage laws, we have:

$$V_{ef} - L\frac{di}{dt} - iR = 0$$

By taking the equations (1)-(4) into consideration, the overall expression of the generator should be:

$$k_e \frac{d\theta}{dt} - \frac{L}{k_t}\frac{d}{dt}\left(\tau_m - J_m \frac{d^2\theta}{dt^2}\right) - \frac{R}{k_t}\left(\tau_m - J_m \frac{d^2\theta}{dt^2}\right) = 0$$

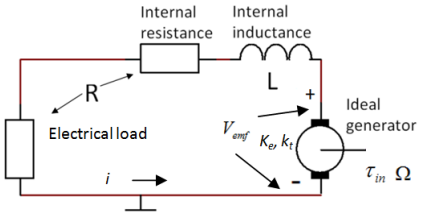

Figure 4. 6 Model of the electromagnetic generator

The inertia of the motor J_m will be considered together with the transmission as an equivalent mass in the following. The transmission parts including rack-pinion, clutches, bevel gears and planetary gears can be taken into consideration together with a transmission ratio of i_t and efficiency of η_t.

$$i_t = \frac{1}{r} k_h k_b$$
$$\eta_t = \eta_r \cdot \eta_{cl} \cdot \eta_b \cdot \eta_p$$

where k_h and k_b are the transmission ratio of the planetary gear head and the transmission ratio of the bevel gears, r is the radius of the pinion gears, and $\eta_r, \eta_{cl}, \eta_b$ and η_p correspond to the efficiency of rack-pinion, roller clutch, bevel gears and planetary gears, respectively.

By taking the inertias of the motor J_m, planetary gear head J_g and the larger bevel gears J_b into consideration, we can use an equivalent mass *at the end of the rack* to represent them.

$$m_s = \frac{J_m k_h^2 k_b^2 + J_g k_b^2 + J_b}{r^2}$$

Note that the above equation we didn't take the inertia in oscillatory motion into account, including those of the shaft, pinion gears, and rack, which act differently from the inertia in unidirectional rotation. When the shock absorber is mounted in a vehicle, the inertia in oscillatory motion will be connected with the chassis or wheel rigidly. Considering such a inertia is much smaller than chassis inertia, the influences of the oscillating inertia are neglected.

4.3.2 Circuit based modeling

A circuit based modeling method is implemented to simulate the dynamic properties of the regenerative shock absorber. Perter C. Breedveld[27] introduced the concepts of effect and flow, which can be used to solve the multi-domain problems with the uniform format.

In this case, the regenerative shock absorber involves both mechanical and electrical domains. So it would be easier to analyze the system after transferring the mechanical elements into electrical elements.

Table 4. 1 Corresponding elements in different domains

Mechanical element (linear)	Mechanical element (rotational)	Electrical element
Force	Torque	Voltage
Velocity	Rotation speed	Current
Spring	Rotation spring	Capacitor
Damper	Rotation damper	Resistor
Mass	Inertia	Inductor

Due to the engagement and disengagement of the roller clutches, the dynamics of the energy-harvesting shock absorber is not linear. The dynamics of such nonlinear mechanical motion system appears to be very complicated. However, if we think more about the physical insights, we can model the system by make an analogy between mechanical motion rectifier and electrical voltage rectifier.

Figure 4.7 shows the overall modeling of the proposed regenerative harvester system. Different from the typical center-tapped transformer with one primary coil and two

secondary coils, in this modeling we have two primary coils and one secondary coil, where the two larger bevel gears correspond to two primary coils and the smaller bevel corresponds to the secondary coil. The two roller clutches between the shaft and the two larger bevel gears correspond to the two semiconductor diodes. The shaft is driven by the rack pinion. Only one larger bevel gear is driven in positive or negative half cycles, in a manner similar as the electrical current flow through only one primary coil. And the unidirectional rotation will occur in the smaller bevel gears, as the DC current exists in the secondary coil. Therefore, the irregular oscillatory vibration is converted into the regular unidirectional rotation by the proposed mechanical motion system. The mechanical impedance (torque from the generator and electrical load by the rotation speed) acts as the electrical impedance in the electrical circuit. Hence, we can use the well-developed principle of AC/DC power electronics [28] to model the nonlinear mechanical motion rectifier system. Note again that this motion rectifier is to regulate the motion, not just a substitute of electrical voltage rectifier.

Other elements of the regenerative shock absorber are treated as follows:

1) The DC motor can convert the electrical energy into mechanical energy. Also it can convert mechanical energy into electrical energy. It is treated as a gyrator in the circuit-based modeling,

$$U = k_e \cdot \omega \tag{9}$$

$$\tau = -k_e \cdot \frac{k_t}{k_e} \cdot i = \eta_g \cdot k_e \cdot i \tag{10}$$

where the gyration resistance $R = k_e$, efficiency $\eta_g = \frac{k_t}{k_e}$.

2) The transmission ratio including rack-pinion $\frac{1}{r}$, bevel gear ratio k_b and plenary gear head k_h is modeled as an ideal transformers or DC-DC converters with the a gain the same as the transmission ratio $i_t = \frac{1}{r} k_h k_b$. The “ideal transformer” can be used either as a transformer or as a DC-DC converter.

3) The two roller clutches are modeled as diodes where the forward voltage drop corresponds to the friction force. The subsystem can be modeled as a full wave rectifier.

4) The viscous damping in the mechanical system can be modeled as peristaltic resistors, but for this case, the mechanical damping is comparatively small, so they are omitted and not shown in the overall model.

5) The internal inductances of the generator are comparatively small, which can be neglected.

In this way the overall system can be modeled as a circuit in Figure 4.7 (a).

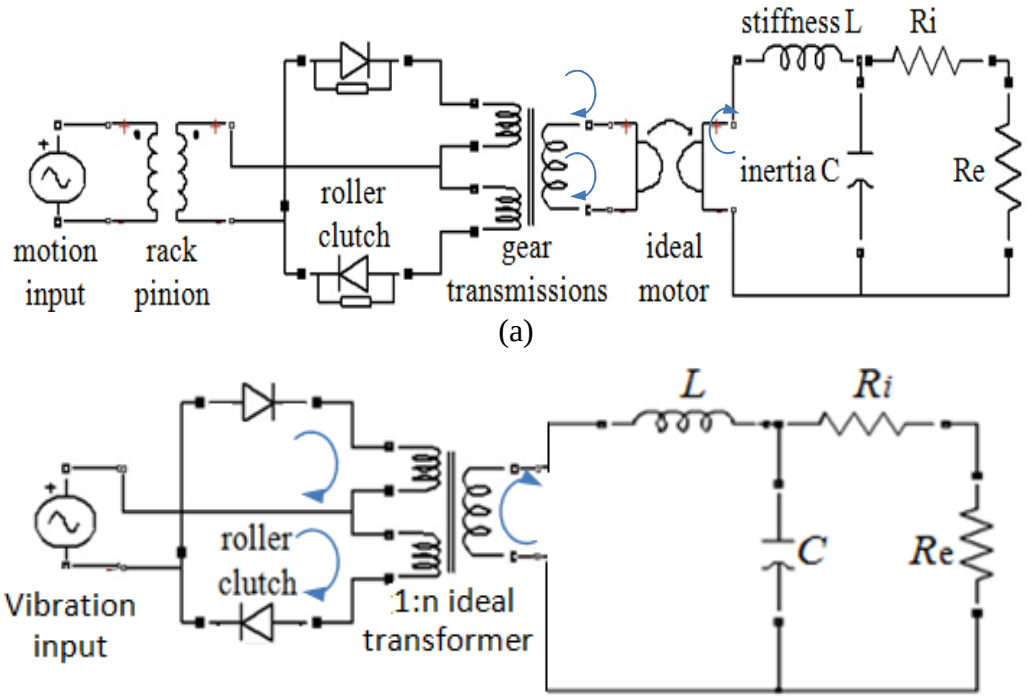

Figure 4. 7 Modeling for regenerative shock absorber using electrical circuit: (a) original, (b) simplified

We can further simplify the system to Figure 4.7 (b). The value of the electrical components (for simplified circuit model) can be decided with the system's mechanical properties as the following:

Inductor $L = \frac{k_h^2 k_b^2 k_e k_t}{r^2}\frac{1}{k_s} + L_i$

Capacitor $C = \frac{1}{k_e k_t} m_s$

Transformer ratio $n = \frac{1}{r} k_h k_b k_e$

where m_s is the equivalent mass expressed in Equation (8), L_i and R_i are the internal inductance and resistance of the generator, and k_s is the stiffness of the mechanical structure, including gear teeth, shafts, etc.

4.3.3 Simulation

Based on this circuit based modeling method, simulations can be done with Simulink/MATLAB. Figure 4.8 shows that the output voltage of the generator under vibration of different frequencies. We see that the voltage is smoother when the input frequency is higher, since the effect of the motion inertia is larger at higher frequencies.

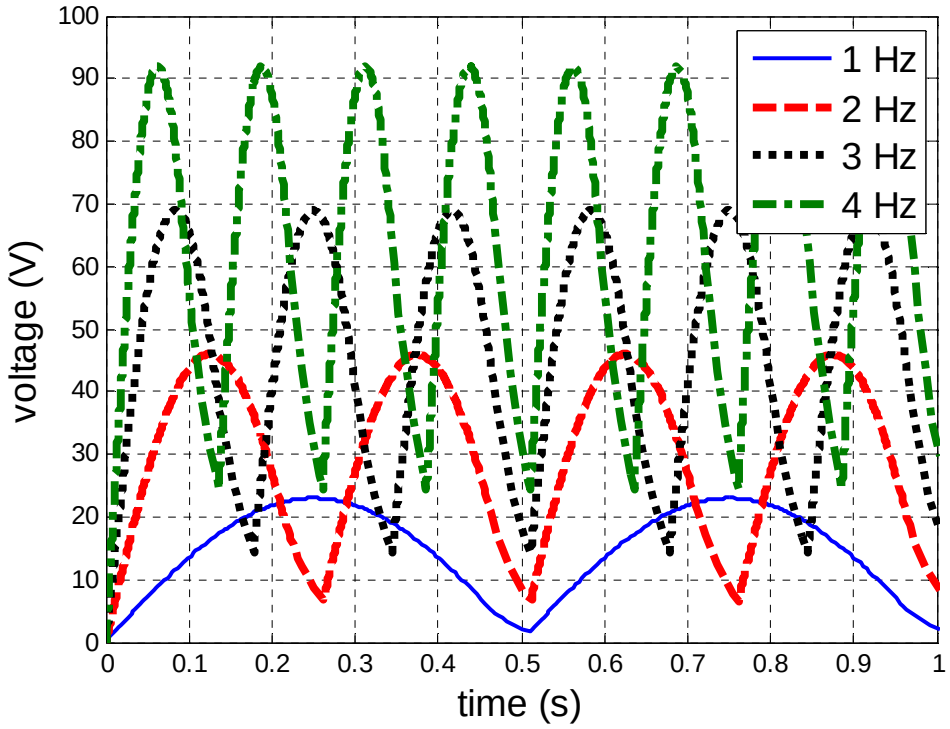

Figure 4. 8 Voltage simulation for excitations at different frequencies with electrical load $R_i+R_e= 100\ \Omega$

The simulated voltages under different electrical load are shown in figure 4.9. It can be seen that the voltage is steadier with larger electrical resistors. This phenomenon is similar as that in voltage rectifier, where smaller electrical resister needs larger smoothing capacitor to maintain a steady voltage.

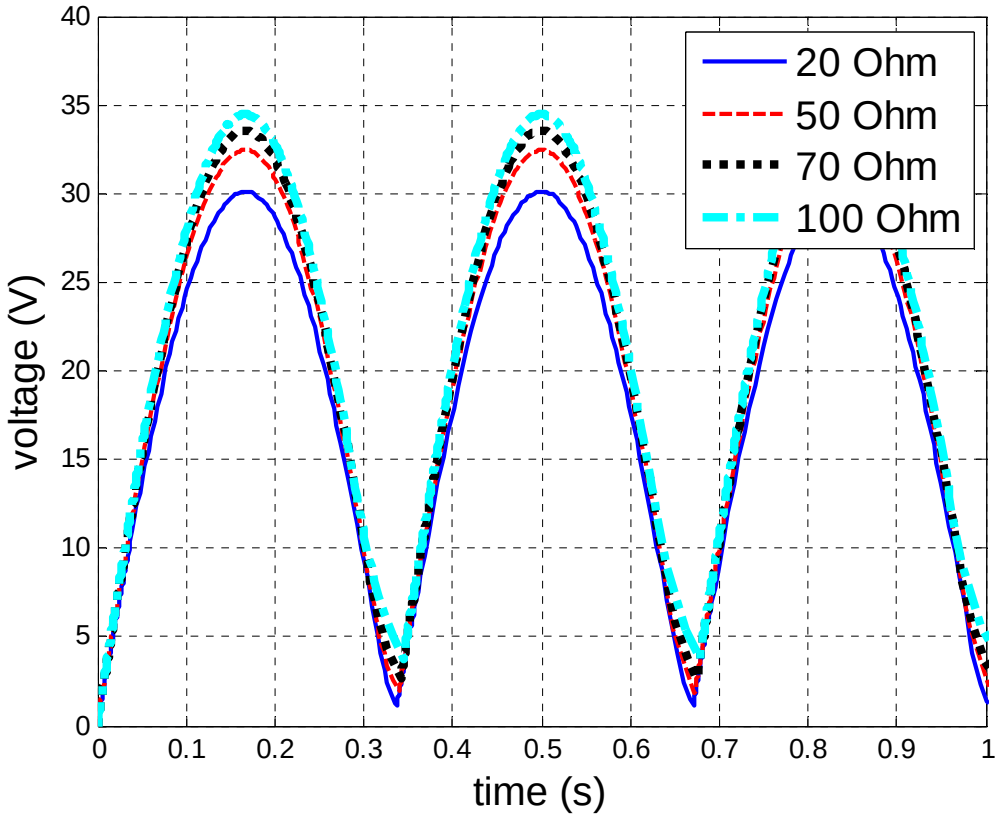

Figure 4. 9 Voltage simulation for different total electric loads at 1.5 Hz

4.4 Experiments and results

4.4.1 Experiment Setup

The prototype was tested with the MTS 858 Mini Bionix II testing system and a dynamic signal analyzer (Hewlett Packard Model 35670A), which are showed in figure 4.10. We use a sinusoidal input with comprehensive range of frequencies and power resistors to run the tests. A strain gauge was attached to measure the force variation corresponding to the displacement of the rack. The motor was hooked up to a resistor which was then connected to a dynamic signal analyzer allowing for the recording of voltage output over time. The experimental test accurately evaluated the performance of the prototype because it provided us with realistic input parameters and substantial amount of highly reliable data.

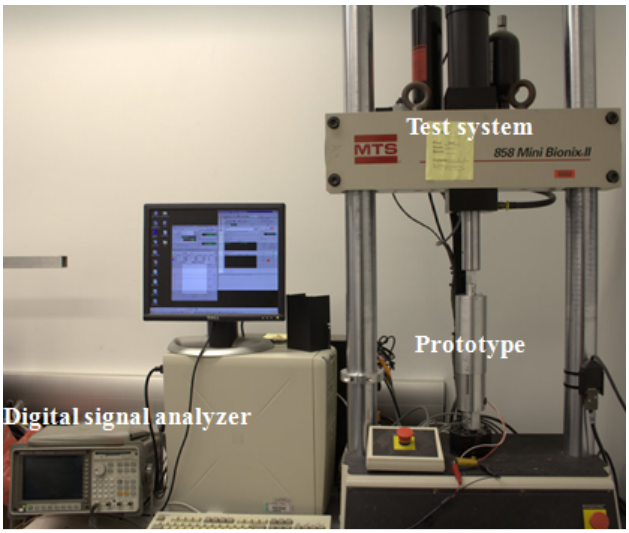

Figure 4. 10 Complete experiment configuration for our regenerative shock absorber

4.4.2 Force-Displacement Damping Loops

Figure 4.11 is the force-displacement damping loop under harmonics excitations. The area of the loop means the mechanical work input of the shock absorber in one cycle. When there is not resistor connected (open circuit), the damping loop area is contributed by the mechanical loss such as frictions. The loop of open circuit is comparatively small, which means that the friction's work is small and high efficiency can be expected. In this figure, the forces came to zero before the displacements reach to maximum or minimum. This is because the kinetic energy stored in the motion inertia m_s is returned to the system and the roller clutch was disengaged.

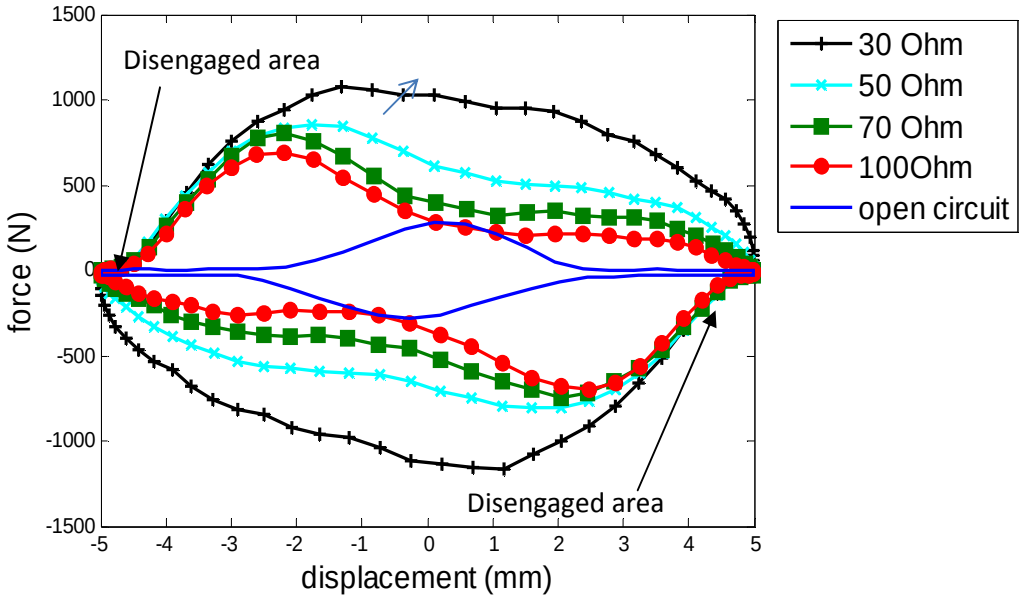

Figure 4. 11 Damping loops for different external electrical loads under vibration input of 1.5 Hz and 5mm amplitude

Since the suspension vibration is in broad spectrum, mainly 1-10Hz, we also investigated the performance at different frequencies. Figure 4.12 shows the damping loops at various frequencies. The results indicate that at higher frequency the disengaged area is larger which corresponds to larger energy storage effect of motion inertia. The engagement and disengagement behaviors can be seen clearly in the recorded force during one cycle in Figure 4.13. It is interesting to observe that at low frequency the force reaches its maximum before the input velocity reaches the maximum, and at high frequency the force reach its maximum after the input velocity reaches the maximum. It is also noted that at high frequency the force is not zero when the displacement reaches the ends (input velocity reaches zero). The reason is the inertia force since the total force is composed on the back electromotive force proportional to the generation speed, the inertia force to accelerate the moving inertia, and possibly some friction. Note that the input force cannot decelerate the inertia in unidirectional rotation because the roller clutches.

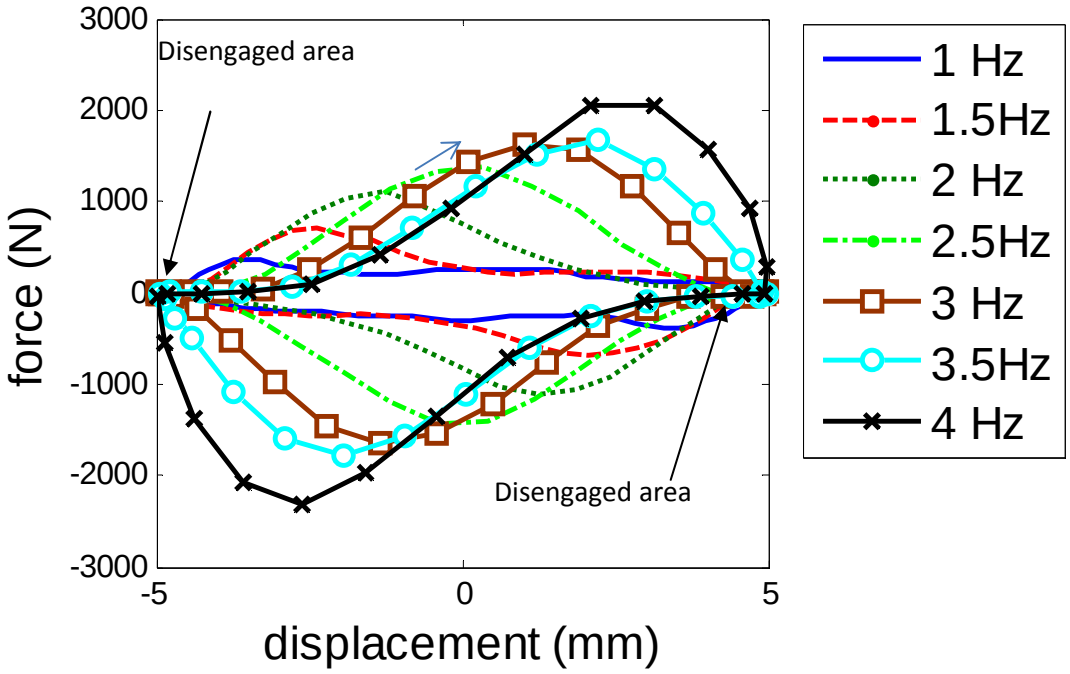

Figure 4. 12 Damping loops for different input frequencies with electrical load R_i+R_e= 106.6 Ω

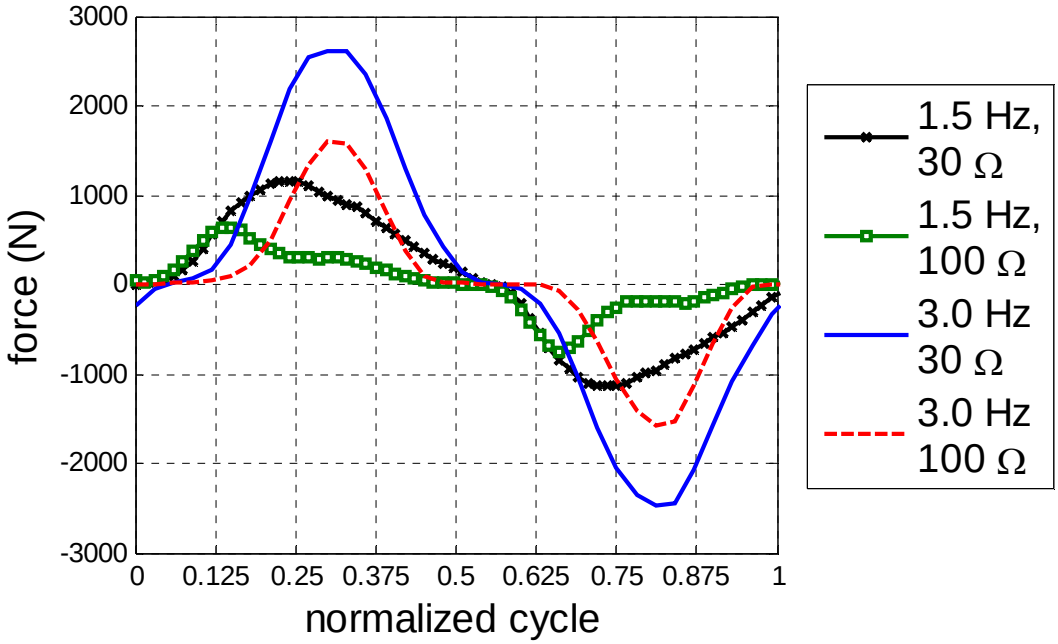

Figure 4. 13 Measured force in one cycle for 30 Ohms and 100 Ohms external resistive loads under 1.5 and 3.0 Hz vibration inputs of ±5mm displacement.

4.4.3 Energy Harvesting and Efficiency

Figure 4.14 shows the input recorded voltage on the external resistors of 23.4 and 94.6 Ohms (internal resistor 6.6 Ohms) under harmonic excitation of 3Hz and 5mm amplitude. The recorded input velocity is also shown in Figure 4.14 as comparison (root mean square 0.047m/sec). Since the regenerated voltage is proportional to the output velocity of the generation, this Figure 4.14 actually illustrated the relationship of input velocity and output velocity of the mechanical system, which is the motion rectification. We can also find from Figure 4.14 that the peak voltage is lower at smaller electrical load, as predicted in the simulation Figure 4.9. However, compared with Figure 4.9, the measured voltages after the valleys didn't rise as sharp as the simulation, which might because of the engagement of the roller clutch takes some time.

The electrical power can be calculated based on the voltage and resistive electrical load. Figure 4.15 shows output electrical power achieved with 3 Hz 5mm displacement input on 100 Ohms and 30 Ohms electrical load. It can be seen that at root mean square 0.047m/sec we harvested the peak power 62.9 Watts and 104.3 Watts, and average power 25.6 Watts and 40.4 Watts at the 100 Ohms and 30 Ohms electrical load, respectively.

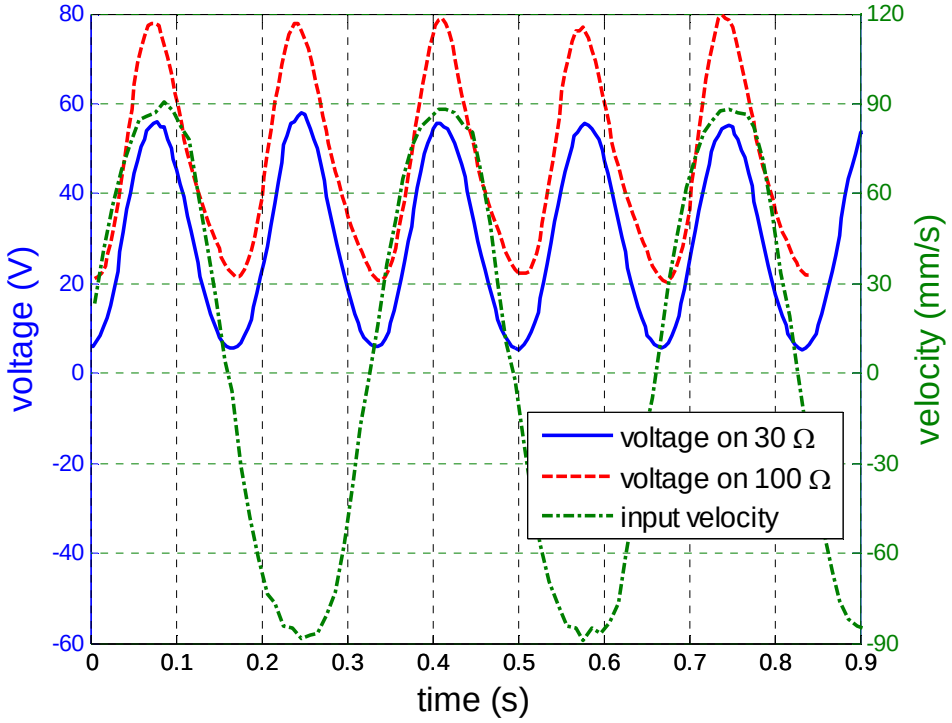

Figure 4. 14 Measured output voltage on 30 and 100 Ω external resistive loads (total 36.6 and 106.6 Ω) under 3Hz 5mm vibration excitation, in comparison with the measured input velocity.

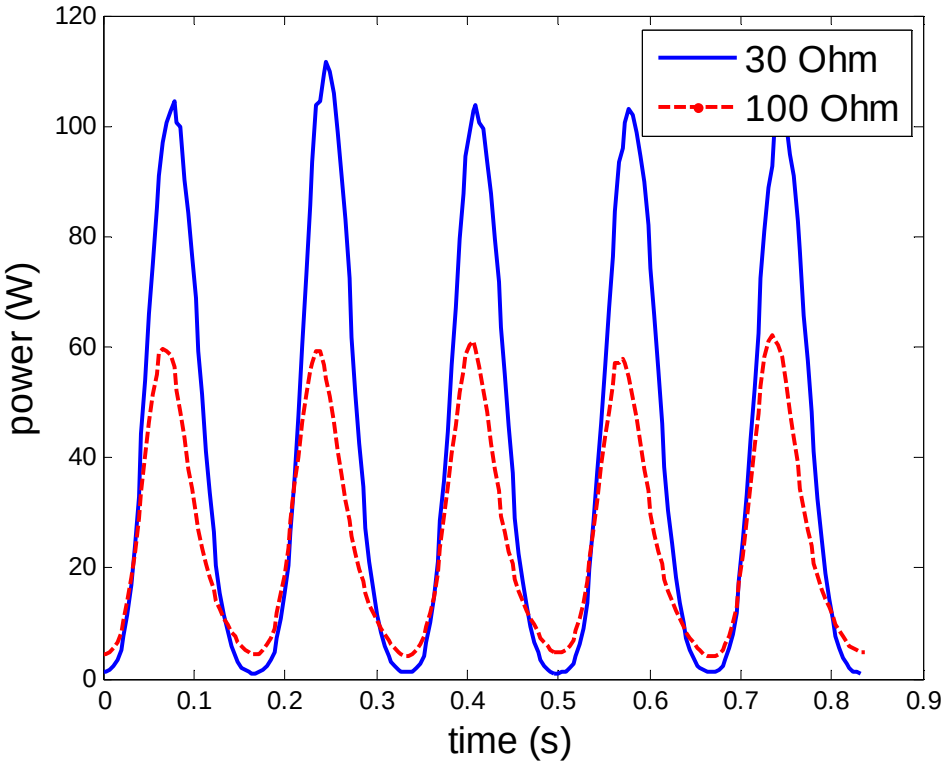

Figure 4. 15 Measured output electrical powers on 23.4 and 93.4 Ω external resistive loads (total 30 and 100Ω) under 3Hz vibration input, where the average powers achieved is 40.4 Watts and 25.6 Watts under rms velocity 0.047m/s.

Based on the mechanical work in cone force-displacement cycle and electrical work on the external resistor, the total efficiency of the system will be obtained, which can be decomposed of electrical efficiency η_e and mechanical efficiency η_m. The electrical efficiency is the ratio of power on external electrical load and total electrical power, which is the external load resistance R_e divided by the sum of external and internal resistance R_e+R_i. The R_i of our generator is 6.6 Ω, the electrical efficiency η_e is 82%~94% for R_e=30~100Ω. The mechanical efficiencies at different electrical load R_i+R_e under 1.5Hz and 5mm amplitude vibration are shown in Figure 4.16. From this figure, we can find that the mechanical efficiency is around 60%. And mechanical efficiency η_m increases when the electrical resistor *R*e decreases.

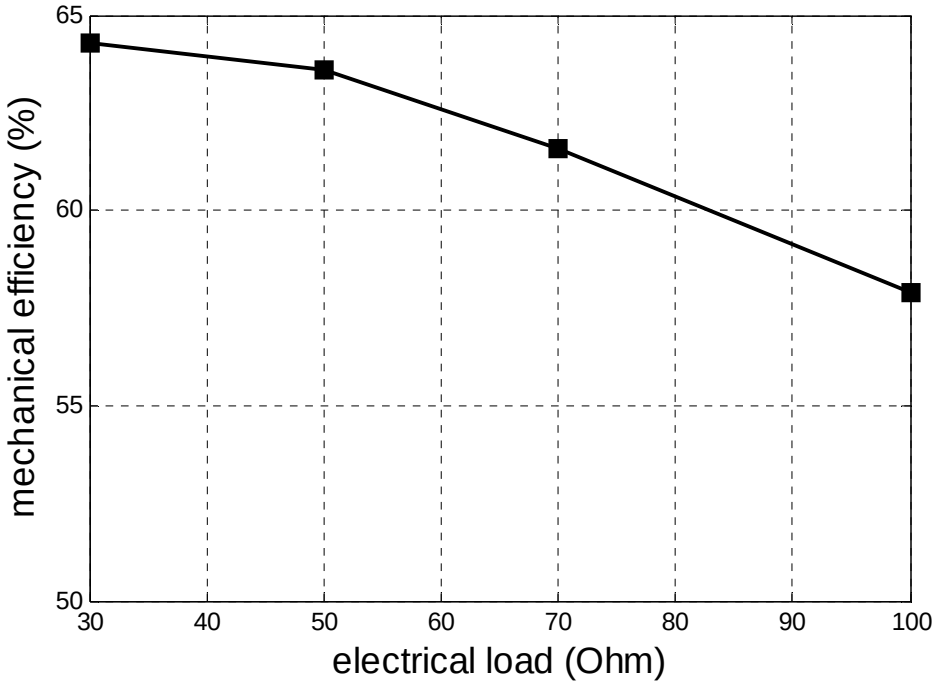

Figure 4. 16 The mechanical efficiencies at different electrical loads under 1.5 Hz and 5mm vibration input.

The mechanical efficiencies at different vibration frequencies are plotted in Figure 4.17. From the figure, we can see that the efficiency tends to increase with the increase of frequency in some range. When the frequency rise up to some point, the efficiency achieves some steady value, which is around 62% in our prototype. Compared with the results of conventional regenerative shock absorber in oscillatory rotation [18], the efficiency is significantly improved at higher frequency (from 30-45% to 62%). Due to the constraint of the hydraulic test machine, we were not able to test at even higher frequencies.

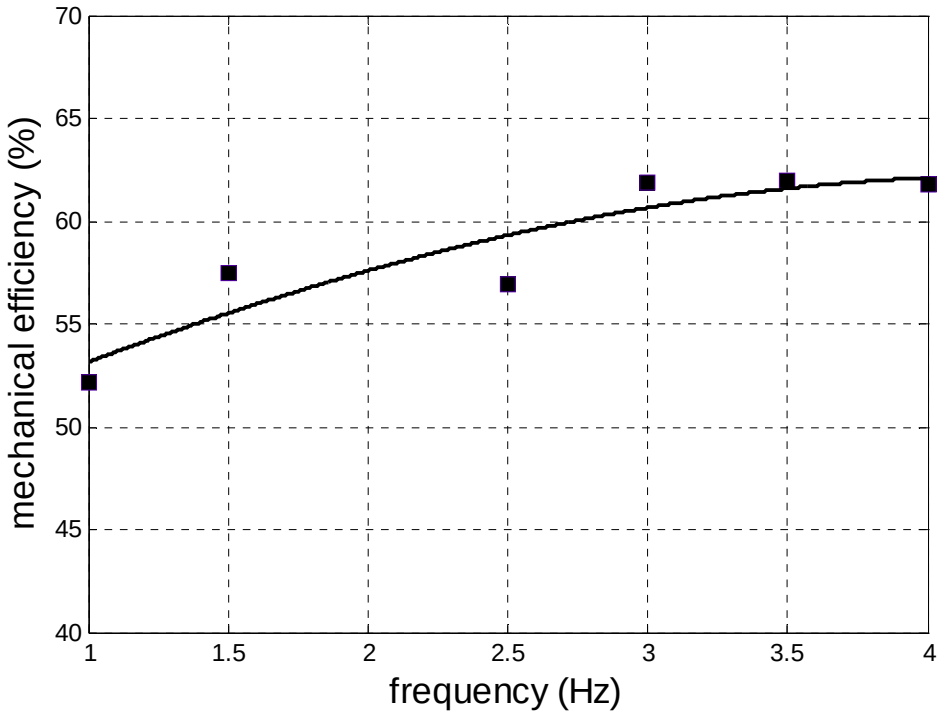

Figure 4. 17 The mechanical efficiencies with different vibration frequency, where electrical load is R_l+R_e= 100 Ω and vibration amplitude is 5mm.

In addition to the bench tests in the lab, we also did some road tests to verify the feasibility the principle and design. Our MMR shock absorber was installed on a Chevrolet Suburban SUV (figure 4.18) to replace its the left rear shock absorber. The displacement and electric output power is showed in figure 4.19. With 20 Ohm's external electrical load, the average output power was 15.4 Watts when the vehicle was driven at 15 mph on the circle road of State University of New York at Stony Brook. The result gives us the most convincing evidence that the MMR shock absorber is feasible for energy harvesting from vehicle suspensions.

Figure 4. 18 The road test setup for the MMR shock absorber, (a) test vehicle Chevrolet Suburban SUV, (b) measurement equipment in the vehicle. (c) MMR shock absorber mounted on the left rear suspension.

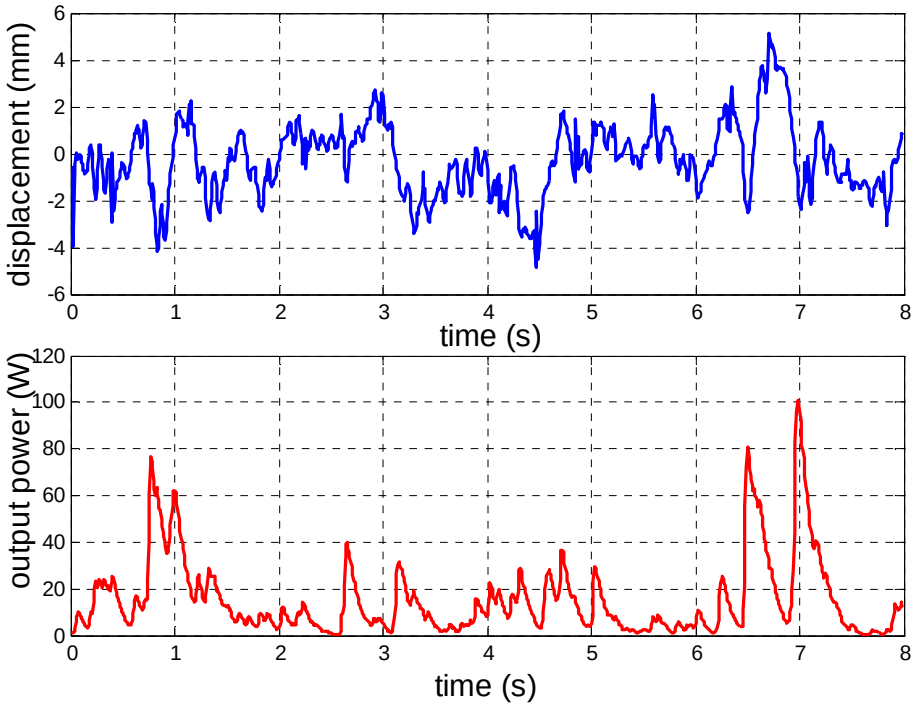

Figure 4. 19 The road test results of displacement and output electrical power with 15 mph on campus road

4.5 Conclusions

In this chapter, we proposed a “motion rectifier” based design of electromagnetic energy harvester for enhanced efficiency and reliability for potential application of vibration energy harvesting from vehicle suspensions. “motion rectifier” can transfer the oscillatory motion of vehicle suspension into unidirectional motion of the electrical generator, thus enabling the generator operating in a relatively steady speed with higher efficiency. In such a design, the motion inertia will act as a filtering capacitor to temporarily storage the energy and smooth the rotation, which can decrease the influences of backlash impact and static friction.

An innovative implementation of the motion rectifier is introduced with high compactness and improved efficiency. The roller clutches are embedded in two bevel gears and the function of “motion rectifier” is achieved with three bevel gears. In addition, the mechanical-electrical system of the regenerative shock absorber is modeled with a circuit-based method to analyze the dynamic properties of the system. Finally the shock absorber is characterized with bench tests. The “motion rectifier” based design achieved a mechanical efficiency of over 60% and no obvious backlash effect. It also harvested average powers 40.4 Watts and 25.6 Watts on 23.4 and 93.4 Ω external resistive loads under vibration of RMS velocity 0.047m/s. The simulation and experiment results indicate that advantage of “motion rectifier” is more important with higher input frequency, and the efficiency is higher correspondingly. Furthermore, the feasibility of this principle and prototype is verified by road tests, in which 15.4 Watts power are obtained at 15 mph on a local road.

Chapter 5 ball screw based regenerative shock absorber with mechanical motion rectifier

Considering that the rack and pinion mechanism cannot be designed to handle large load in very limited space, we choose to use ball screw to transfer the linear motion into rotational motion. Also, we found that the mechanical motion rectifier(MMR) can significantly improve the dynamic performances of the mechanical structure, a combination of ball screw and MMR would a great solution for the regenerative shock absorber.

5.1 Design introduction

This design makes use to two ball screw nuts to convert linear bi-directional motion to one directional rotational motion. This rotational motion is kept in one direction with the use of roller clutches. Angle Bearings are used to handle the radial and axial forces on the mechanism due to vibrations.

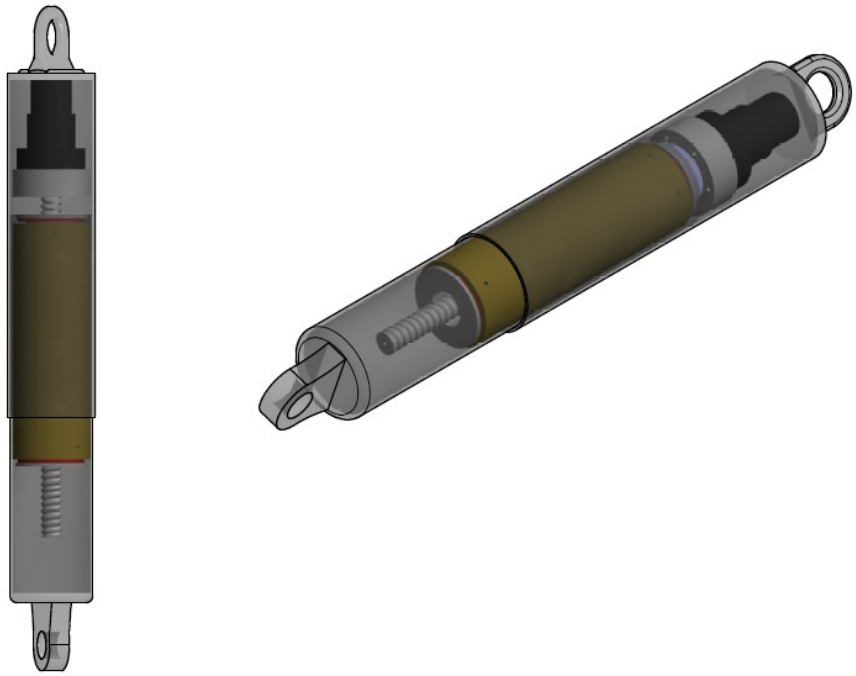

Figure 5. 1 A design of ballscrew based MMR regenerative shock absorber

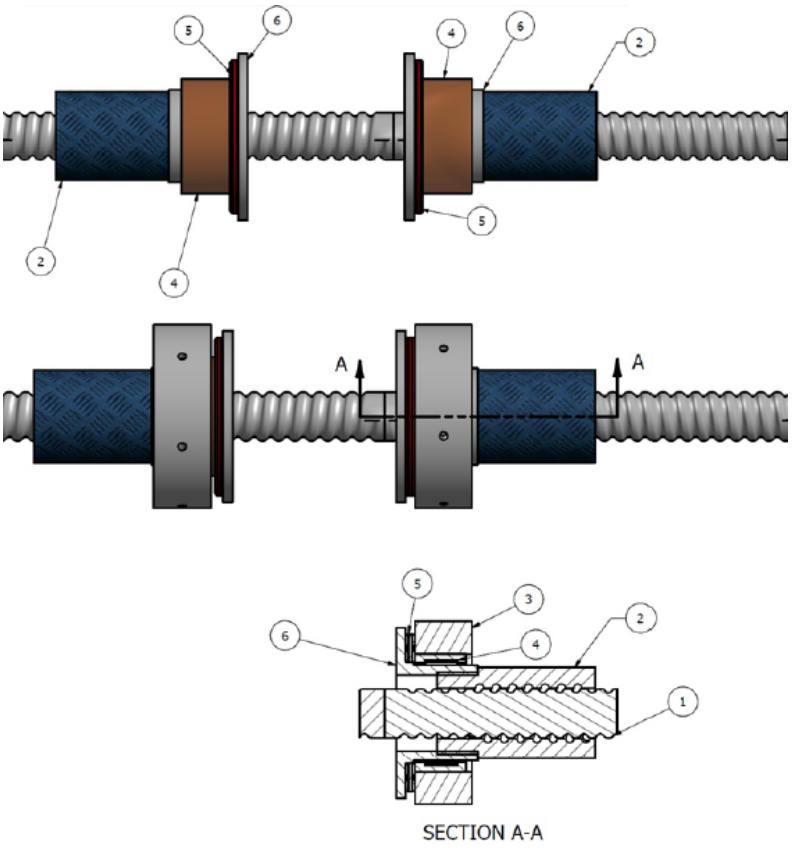

Figure 5. 2 The inner structure of the ballscrew based MMR shock absorber

The teeth on the ball screw shaft is alternated at two sections to provide one directional rotation with up and down motion of the ball screw nuts at those sections. For example if the desired rotational motion is counter-clockwise and down-ward motion of the ball screw nut on the upper half of the half provides this motion. Then the roller clutch at this point locks. However the roller clutch with the ball screw nut at the bottom half of the shaft does not lock because down-ward motion in this section provides clockwise rotation. And the counter-clockwise motion is transferred to the generator from the upper half. In addition, the bottom nut will also have a "compensation rotation", which means it rotates to follow the linear motion of the other nut.

Then with up-ward motion the reverse occurs, where counter-clockwise rotational motion is utilized from the bottom half of the shaft and the rotation of the upper half is "compensation rotation".

The overall system works by converting bi-directional linear motion into one directional motion. This motional conversion was our main problem in the design throughout the course of our project and we came up with the solution for this. By utilizing a ball screw assembly, with alternating thread direction (RH/LH) on the screw shaft together with the use of uni-directional roller clutches, we were able to control the motion. The two linear motions we had to control were the Upward and Downward motion respectively.

5.1.1 Downward Motion

As the hollow shaft moves down-ward, the roller clutch #1 on the inside of it moves down-ward as well. The ball screw nut #1 inside roller clutch #1 will move in the same direction too. However, based on the ball screw mechanism the nut will try to rotate clockwise as it moves downward. But the roller clutch #1 locks for rotational motion in the clockwise direction, keeping the ball screw nut #1 in a linear down-ward motion. This linear down-ward motion of the ball screw nut # 1 will cause the ball screw shaft to rotate in the counter-clockwise direction. And since the generator is connected directly to the ball screw shaft, it will rotate in the counter-clockwise direction to harvest electrical energy.

For ball screw nut #2, down-ward motion will cause it to rotate in the counter-clockwise direction. And it is allowed to rotate freely counter-clockwise because roller clutch #2 over-runs in that that direction.

5.1.2 Upward Motion

As the hollow shaft moves up-ward ball screw nut #1 is allowed to over-run in the counter-clockwise direction by roller clutch #1. However, roller clutch #2 locks for clockwise rotation of ball screw nut # 2, which moves the nut linearly up-ward, resulting in the counter-clockwise rotation of the ball screw shaft. The same result as down-ward motion is obtained as the generator rotates in the counter-clockwise direction.

Note: The ball thrust bearings are put in place to cancel out any thrust and radial forces on the ball screw shaft.

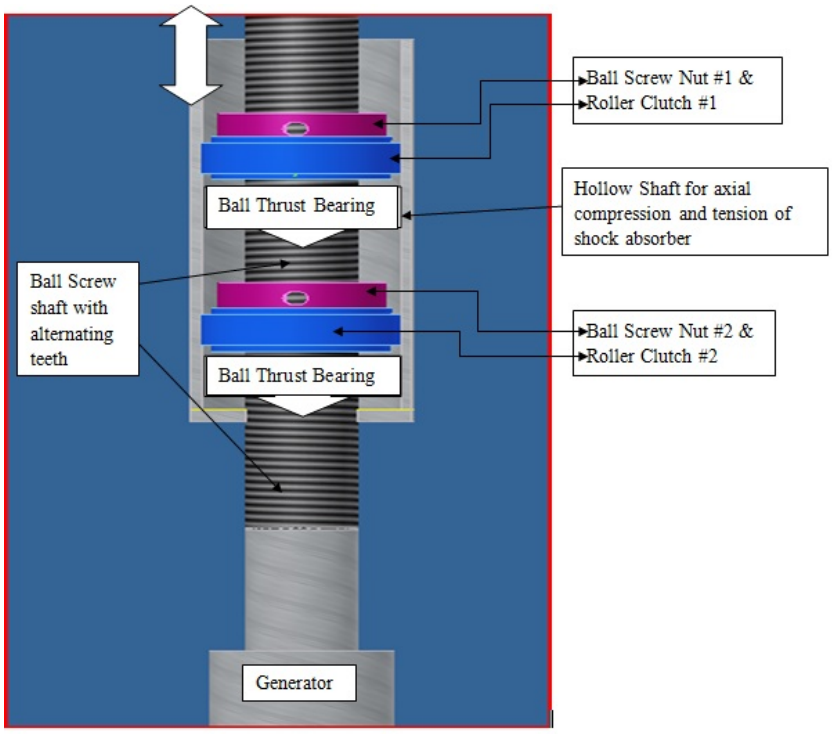

Figure 5. 3 The working principle of ballscrew based Mechanical Motion Rectifier

5.1.3 Properties of ballscrew based MMR

Advantage:

Utilizes a single shaft for higher efficiency;

Ball Screw Mechanism provides low friction-high speed;

Converts bi-directional motion to one directional motion;

Utilizes a small space inside the shock absorber.

Disadvantage:

Each ball screw nut must remain in specified section of the shaft;

The structure is more complicated and it needs more precision.

5.2 Design of ballscrew base MMR regenerative shock absorber

The components we would use in our design were ball screw, clutch, bearing, and motor. In order to make a correct selection, we need to calculate the parameters for each component based on our specifications.

Design Specifications:

Normal velocity: $v = 3.94 \frac{in}{s}$.

Normal Force is: $P = 115lb$.

Frequency range is: $1 \leq f \leq 10$ Hz

Stroke: $s \geq 4$ in.

Over diameter: $d \leq 3$ in.

Load support-factor: Fixed $-$ Fixed: $\lambda = 4.0$.

Required Life: 6 years.

5.2.1 Ball Screw

Ball screw was the major part of the system. It must have short response time, low friction, and will not break during normal use. There are lots of types of ball screw based on different standard. They have various standards because of their threads. We chose to use a ball screw in United States Standard. And its thread was shown as figure 5.4.

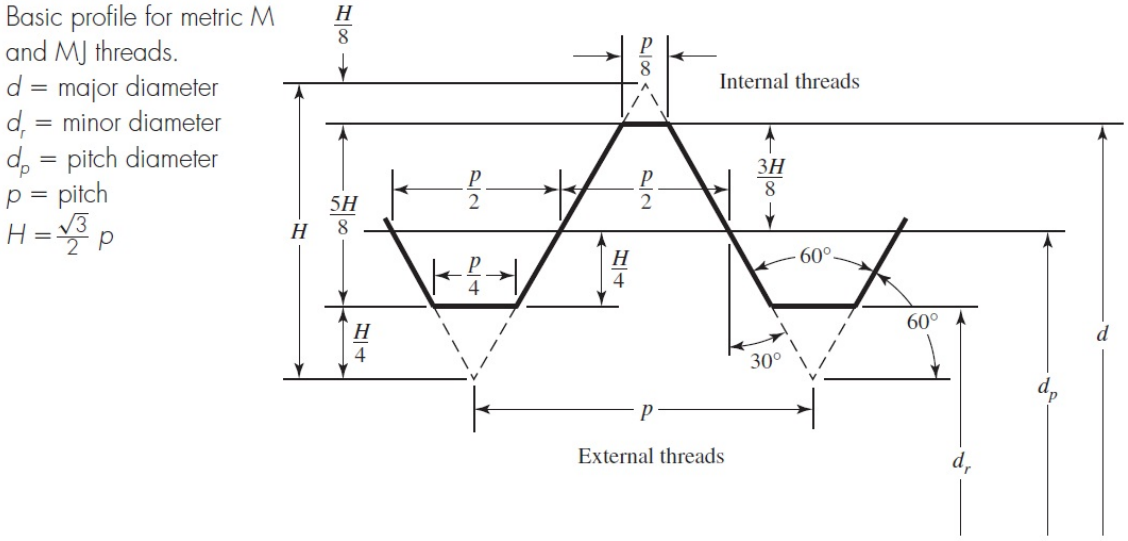

Figure 5. 4 Ball Screw Thread design

The reason of using this standard is that it can handle large load and it is easy to manufacture.

In order to select a best type of ball screw, we made the diameter as 1in as our first attempt with 0.2 in pitch, and stroke is 4 in. Based on these assumptions, both the minor diameter and pitch diameter could be defined as below:

Minor diameter:

$$d_r = d - 1.299038p = 1\ in - 1.299038 \times 0.2 = 0.74\ in$$

Pitch Diameter:

$$d_p = d - 0.649519p = 0.87\ in$$

In the following, we calculated the ball screw life, thrust load, dynamic axial load, lead, RPM, critical speed, etc. All of these parameters would help us to have a best solution.

i. Determine Required Life (inches):

$$Life = 4\frac{inch}{stoke} \times 2\frac{stokes}{cycle} \times 36000\frac{cycles}{hour} \times 3\frac{hours}{day} \times 365\frac{days}{year} \times 6year$$

$$Life = 1{,}892{,}160{,}000\ in$$

ii. Determine Thrust Load on Ball Screw

$$F_a = P \times \mu$$

where P is load applied on the ball screw, and μ is the coefficient of sliding friction. In our system, the load is 115lb, and the coefficient of friction is 0.2. The thrust load was:

$$P_t = 115\ lbf \times 0.2 = 23\ lbf$$

iii. Determine Required Dynamic Axial Loading to Achieve Required Life:

The formula for rated load (P_r), actual load (P_t), and life of assembly under actual load (Life) can be defined as:

$$\left(\frac{P_r}{P_t}\right)^3 \times 1{,}000{,}000\ in = Life$$

Substitute the value we had, the rated load can be calculated as:

$$P_r = \sqrt[3]{\frac{Life}{1{,}000{,}000}} \times P_t = \sqrt[3]{\frac{1{,}892{,}160{,}000\ in}{1{,}000{,}000in}} \times 23lbf = 284.5\ lbf$$

iv. Determine the Lead of Screw:

Lead can be calculated as number of thread multiple by pitch, which was:

$$l = np$$

where l is lead, n is number of thread, and p is pitch. We would use single thread, which means n=1. The lead was:

$$l = np = 1 \times 0.2\ in = 0.2\ in$$

v. Determine the RPM of Ball Screw:

The relationship for lead, velocity and revolution is:

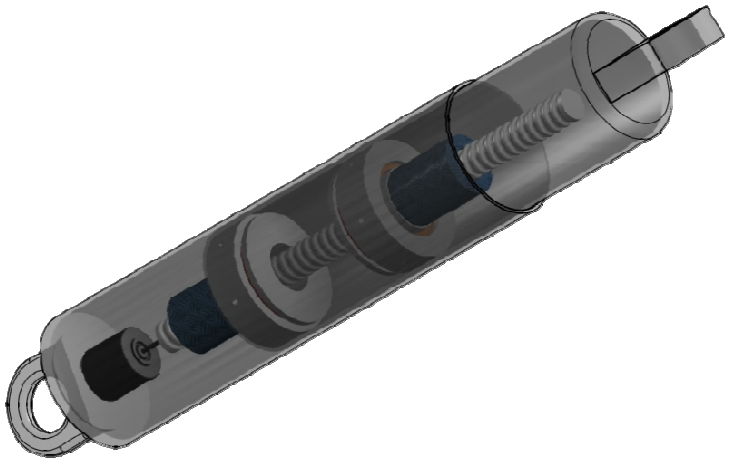

Figure 5. 5 3D model of the overall prototype

5.2.2 Design restriction

The ballscrew based motion rectifier can generate unidirectional rotation by the different engaging cycle of the roller clutches. At each cycle, one nut is driving the screw shaft and the other is driven by the shaft. However, under some circumstance, the nut might not be driven no matter how large force the shaft is driving.

In order to explore the restriction of this design and provide some guidelines for future designs, I created an abstract model to analyze the problem.

The ball screw mechanism can be projected in 2D surface as an object on a slope. And the angle between the slope and the horizontal line is the lead angle . Besides, the bottom block represents the thrust bearing.

Suppose the ball screw mechanism's friction coefficient is , and the friction coefficient of the thrust bearing is .

So if we want the ball screw to can be driven under this condition, it has to satisfy:

where

$$f_b = \mu_b N_b$$

$$f_t = \mu_t N_t$$

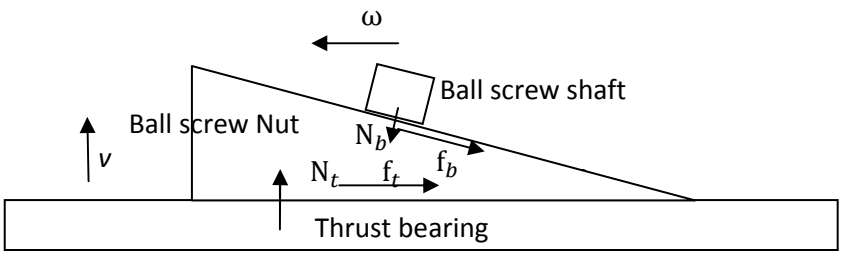

Figure 5. 6 Diagram of the ballscrew MMR system

So, based on the inequations above, the design requirement for this structure is

$$\tan\theta > \frac{\mu_t + \mu_b}{1 - \mu_t \mu_b}$$

5.3 Conclusion

An innovative design of ball screw based MMR regenerative shock absorber is designed and analyzed. The linear oscillation motion of the vehicle suspension can be transferred to rotational, unidirectional and smoothed motion, which can benefit the regenerative shock absorber with better efficiency and better reliability.

Ball screw MMR can stand more force and more impact than rack pinion based MMR. However, ball screw based MMR's working principle is more complicated than rack and pinion based MMR. It needs more concern while designing because it has a dead zone, that is, it can never be driven if some parameters are not properly designed.

In this chapter, the dead zone is analyzed with a kinetic model and some design guidelines are given for future designs.

Chapter 6 summary and future work

6.1 Summary

The author first introduced the background on vehicle suspensions and reviewed the development of regenerative shock absorbers. The waste energy recovery from vehicle suspensions is more and more important now and the research on regenerative shock absorbers has started since 1970s. However, the power density is still not good enough for real application and their designs don't have suitable sizes. Besides, no researchers have built their prototypes and test them on the road. Then the author analyzed the potential energy that can be recovered with regenerative shock absorbers based on road test results. It is found that the potential benefits for the vehicle include 1-6% fuel efficiency's increase with better performances.

A rack pinion based prototype is modeled with differential equation based method. The prototype contains rack and pinion gears, bevel gears, a planetary gearbox, and an electrical generator, in which friction, inertia and backlash were considered. The method of differential equations is fundamental and helps in the understanding of the physical characteristics of the system. The physical phenomena of the system such as the "negative stiffness" due to inertia and large impact forces due to backlash under sinusoidal vibration input are explained correctly and precisely by the model. And some guidelines about how to design an energy harvester with improved performance are presented. The relationship between the performance index and design parameters are estiblished through modeling, which can be used to further guide the design of retrofittable shock absorber.

Then a retrofit rack-pinion based electromagnetic regenerative shock absorber is developed and tested. The prototype is tested on a testing machine with sinusoidal displacement input. The results show that the equivalent damping coefficient depends on the external electrical resistances. As a result, the regenerative shock absorber can be used as a controllable damper, and the damping coefficient can be controlled by controlling equivalent external electrical load. A total energy conversion efficiency of 56% is achieved. The regenerative shock absorber could also attain asymmetric performances in jounce and rebound by connecting it with asymmetric load circuits. Road tests were also carried out to verify the performance of the new designed regenerative shock absorber. The experiment results indicate that the generated voltage reflects the road irregularities well. A peak power 270 watts and average power 20 watts can be obtained from four energy-harvesting shock absorbers when the vehicle travels at 30mph on campus road.

Based on the previous analysis on rack and pinion based shock absorber, the author proposed a "motion rectifier" based design of electromagnetic energy harvester for enhanced efficiency and reliability for potential application of vibration energy harvesting from vehicle suspensions. "Motion rectifier" can transfer the oscillatory

motion of vehicle suspension into unidirectional motion of the electrical generator, thus enabling the generator operating in a relatively steady speed with higher efficiency. In such a design, the motion inertia will act as a filtering capacitor to temporarily storage the energy and smooth the rotation, which can decrease the influences of backlash impact and static friction. An innovative implementation of the motion rectifier is introduced with high compactness and improved efficiency. The roller clutches are embedded in two bevel gears and the function of "motion rectifier" is achieved with three bevel gears. In addition, the mechanical-electrical system of the regenerative shock absorber is modeled with a circuit-based method to analyze the dynamic properties of the system. Finally the shock absorber is characterized with bench tests. The "motion rectifier" based design achieved a mechanical efficiency of over 60% and no obvious backlash effect. It also harvested average powers 40.4 Watts and 25.6 Watts on 23.4 and 93.4 Ω external resistive loads under vibration of RMS velocity 0.047m/s. The simulation and experiment results indicate that effect of "motion rectifier" is more important with higher input frequency, and the efficiency is higher correspondingly.

As the ball screws have better reliability than rack pinion mechanism, the author combine the motion rectifier with ball screw and create a ball screw based MMR regenerative shock absorber. The linear oscillation motion of the vehicle suspension can be transferred to rotational, unidirectional and smoothed motion, which can benefit the regenerative shock absorber with better efficiency and better reliability. Ball screw MMR can stand more force and more impact than rack pinion based MMR. However, ball screw based MMR's working principle is more complicated than rack and pinion based MMR. It needs more concern while designing because it has a dead zone, that is, it can never be driven if some parameters are not properly designed. So, the dead zone is analyzed with a kinetic model and some design guidelines are given for future designs.

6.2 Analysis of failure modes and recommendation for future work

6.2.1 Retrofit design failure modes

1. **Worn rack teeth**
2. **Worn pinion teeth**
3. **Broken bevel gear**
4. **Loose bevel gears' engagement**

The reason for No. 1, 2, 3 is that there is too much shock for the structures. The solution would be either to increase the size (strength) of the gears, or change another principle with less shock.

For No. 4 failure, the reason is that the shaft is floating without constraints. And there is only some press force to hold it. So it might move during working, which will change its position and make the engagement loose. So, my suggestions for improvement is to design some stages on the shaft to prevent it from moving, which might make the bevel gears' engagement loose and the backlash become larger.

6.2.2 MMR (rack pinion) design failure modes

1. **Broken pinion teeth & Worn rack teeth**
2. **Broken pin between shaft and pinion gear**
3. **Broken stroke limits**

To improve the MMR (rack pinion) design's reliability, there are several aspects need to be taken care of.

First, the No. 1 mode was caused by the loose bolts/nuts on the motors. all the bolts and nuts should be fastened with enough preload to fix the structures. The flexibility of the structures will cause loose engagement, large backlash, and excessive vibrations. These are very harmful to the structures.

Second, the pin used in between the shaft and pinion gear should be replaced with a solid one. Through experiments, we found that the pin broke in 60 mph road tests.

Finally, the stroke of the shock absorber is still not enough for the Chevy SUV we used before. It should be at least increased by one inch.

Reference

[1] Energy Information Administration Basic Petroleum Statistics, http://www.eia.doe.gov/basics/

[2] Advanced Technologies and Energy Efficiency, http://www. fueleconomy.gov/FEG/atv.shtml

[3]L. Zuo, and S. Nayfeh, Structured H2 optimization of vehicle suspensions based on multi-wheel models. Vehicle System Dynamics, 40(5), 351–371, 2003

[4]OY Abdel-Fattah, SM El-Demerdash, Shock absorber as a contributing cause to motor vehicle accident, 2006 (PDF URL: http://ipac.kacst.edu.sa/eDoc/2006/162305_1.pdf)

[5]K Efatpenah, JH Beno, and SP Nichols, Energy requirements of a passive and an electromechanical active suspension system, Vehicle System Dynamics, Vol 34, n6, 2000

[6] Jones, W.D.; , "Easy ride: Bose Corp. uses speaker technology to give cars adaptive suspension," *Spectrum, IEEE* , vol.42, no.5, pp. 12- 14, May 2005
doi: 10.1109/MSPEC.2005.1402708
[7]L. Segel, X. P. Lu, “Vehicular resistance to motion as influenced by road roughness and highway alignment”, *Australian Road Research*, 1982, 12(4): 211-222.

[8]L. Zuo and P. Zhang, “Energy Harvesting, Ride Comfort, and Road Handling of Regenerative Vehicle Suspensions”, *ASME Journal of Vibration and Acoustics, 2012.*

[9]Zhang, Y., Yu, F. and Huang, K., 2009, “A State of the Art Review on Regenerative Vehicle Active Suspension,” International Conference on Mechanical Engineering and Mechanics, Beijing, pp. 1689-1695.

[10] Karnopp D. Power requirements for traversing uneven roadways[J]. Vehicle System Dynamics, 1978, 7(3): 135-152.

[11] Karnopp D. Power requirements for vehicle suspension systems[J]. Vehicle System Dynamics, 1992, 21(2): 65-71.

[12] Velinsky S, White R. Vehicle energy dissipation due to road roughness[J]. Vehicle System Dynamics, 1980, 9(6): 359-384.

[13] Hsu P. Power recovery property of electrical active suspension systems[C]. Proceedings of the Intersociety Energy Conversion Engineering Conference, Washington, DC, USA, IEEE, 1996: 1899-1904.

[14] Browne A, Hamburg J. On road measurement of the energy dissipated in automotive shock absorbers[C]. Symposium on Simulation and Control of Ground Vehicles and Transportation Systems, Anaheim CA, USA, ASME, 1986: 167-186.

[15] Wendel G. A regenerative active suspension system[C]. SAE International, 910659, 1991.

[16] Fodor M, Redfield R. The variable linear transmission for regenerative damping in vehicle suspension control[J]. Vehicle System Dynamics, 1993, 22: 1-20.

[17] Karnopp, D., 1989, "Permanent Magnet Linear Motors Used as Variable Mechanical Dampers for Vehicle Suspensions," *Vehicle System Dynamics*, **Vol. 18,** pp. 187-200.

[18] Suda, Y., Nakadai, S. and Nakano, K., 1998, "Hybrid Suspension System with Skyhook Control and Energy Regeneration", *Vehicle System Dynamics Supplement*, **Vol. 28**, pp. 619-634.

[19] Goldner, R. B., Zerigian, P. and Hull, J. R., 2001, "A Preliminary Study of Energy Recovery in Vehicles by Using Regenerative Magnetic Shock Absorbers," SAE paper, Washington, D.C.

[20] Ebrahimi, B., Khamesee, M., and Golnaraghi, M., 2008, "Feasibility Study of an Electromagnetic Shock Absorber with Position Sensing Capability," Proc. 34th Annual Conference of IEEE Industrial Electronics IECON, **Vol. 1**, pp. 2988–2991.

[21] Zuo, L., Scully, B., Shestani, J. and Zhou, Y., 2010, "Design and Characterization of an Electromagnetic Energy Harvester for Vehicle Suspensions," *Smart Material and Structures*, **Vol. 19**, pp. 1007-1016.

[22] Martins, I., 2006, "Permanent-Magnets Linear Actuators Applicability in Automobile Active Suspensions", *IEEE Transactions on Vehicular Technology*, **Vol. 55**, pp. 86-94.

[23] Gupta, A., Jendrzejczyk, A. J., Mulcahy, M. T. and Hull, R. J., 2006, "Design of Electromagnetic Shock Absorbers", *International Journal of Mechanics and Materials in Design*, **Vol. 3**, pp. 285-291.

[24] Zhang, Y., Huang, K., Yu, F., Gu, Y. and Li, D., 2007, "Experimental Verification of Energy-regenerative Feasibility for an Automotive Electrical Suspension System," IEEE International Conference on Vehicular Electronics and Safety, Beijing, 2007.

[25] Avadhany, S., Abel, P., Tarasov, V. and Anderson, Z., 2009, "Regenerative Shock Absorber," U.S. Patent 0260935.

[26] Choi, S-B., Seong, M-S. and Kim, K-S., 2009, "Vibration Control of an Electrorheological Fluid-Based Suspension System with an Energy Regenerative Mechanism," *Journal of Automobile Engineering*, **Vol. 223**, pp. 459-469.

[27]Zhang, P. S., 2010, "Design of Electromagnetic Shock Absorber for Energy Harvesting from Vehicle Suspensions," MS thesis, Advisor L. Zuo, Stony Brook University, Stony Brook, NY.

[28] Zuo, L., Tang, X. and Zhang, P., 2010, "Regenerative Shock Absorbers with High Energy Density," U.S. Patent application # 61/368.846.

[29]Kawamoto, Y., Suda, Y., Inoue, H. and Kondo, T., 2007, “Modeling of Electromagnetic Damper for Automobile Suspension”, *Journal of System Design And Dynamics*, **Vol. 1**, pp. 524-535.

[30] Cassidy, I. L., Scruggs, J. T. and Behrens, S.,2011, “Design of Electromagnetic Energy Harvesters for Large-Scale Structural Vibration Applications”, Proc. SPIE 7977, 79770P.

[31] Amati, N., Canova, A., Cavalli, F., Carabelli, S., Festini, A., Tonoli, A. and Caviasso, G., 2006, “Electromagnetic Shock Absorbers for Automotive Suspensions: Electromechanical Design”, ASME 8th Biennial Conference on Engineering Systems Design and Analysis, pp. 131-140.